

Volume 26 Fall 2013

MURJ

Massachusetts Institute of Technology
Undergraduate Research Journal



The world through the eyes of a trauma surgeon p. 12

Nobel Spotlight: Professor Phillip Sharp p. 17

In search of the small cosmological constant p. 27



Now Hiring in North America, Asia, and Europe!

Success Starts Here

As a leading global supplier of wafer fabrication equipment and services to the semiconductor industry, Lam Research develops innovative solutions that help our customers build smaller, faster, and more power-efficient devices. This success is the result of our employees' diverse technical and business expertise, which fuels close collaboration and ongoing innovation.

Join the Lam Research team, where you can write your own success story. Come help us solve our customers' toughest problems and be part of a company that plays a vital role in the future of electronics. We have opportunities for mid-career professionals and new college graduates (Ph.D., MBA, master's, and bachelor's). Lam Research has programs that allow individuals to continue their career development, build on their educational accomplishments, and play key roles in bringing innovative technology and business solutions to market in countries around the world.

Areas of opportunity:

- Business Development
- Chemistry (organic, inorganic)
- Engineering (chemical, computer, electrical, industrial, manufacturing and mechanical)
- Field Operations
- Finance
- Human Resources
- Information Systems
- Legal
- Marketing/Communications
- Materials Science
- Operations/Supply Chain
- Physics
- Plasma Physics
- Program and Project Management
- Quality
- Software Engineering

New College Graduates

Lam Research has programs that allow students to continue their career development and build on their educational accomplishments. We offer new college graduates the opportunity to play key roles in bringing innovative technology and business solutions to market in countries around the world.

College Internships

Lam's internship opportunities offer summer and/or co-op employment for students and provide hands-on business experience that complements academic studies. Students have the opportunity to work closely and learn from some of the best in the industry.

Experienced Professionals

If you are looking for a career in the highest of the high tech industries, join the company that takes you there – Lam Research Corporation. We are looking for the best and brightest to join our team of talented individuals.

For information about specific opportunities, please visit lamresearch.com/careers, where you can also apply online.

Lam Research – a company where successful people want to work

lamresearch.com/careers

EOE/M/F/D/V

MURJ

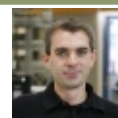
Massachusetts Institute of Technology
Undergraduate Research Journal



Contents

Introductory Letters

From Iain Cheeseman
From MURJ Editors



3-5

Science News In Review

A look at the latest Science News.



6-10

Features



"We Do What We Do": The World Through the Eyes of a Trauma Surgeon

When Michael Yaffe heard about the explosions at the Boston marathon, he rushed to the ER at the Beth Israel Deaconness Medical Center. Yaffe, a trauma surgeon as well as a Professor of Biology and Biomedical Engineering at MIT, spent the next 22 hours operating on blast victims.

12-16



**Nobel Spotlight:
Professor Phillip Sharp, MIT
Department of Biology**

MURJ spoke with Professor Phillip Sharp, who discovered RNA splicing as an assistant Professor at MIT 36 years ago—for which he won the 1993 Nobel Prize in Medicine or Physiology—and has pushed forward biology at an extraordinary clip ever since.

17-20

UROP Summaries

Bio-Inspired Strong-yet-Tough Polymer Composite Reinforced by Water 22-23

Samuel Lim, Mingming Ma,
Robert Langer

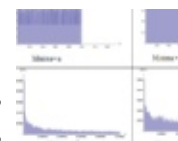
RNAi screen for suppression of epileptic seizure susceptibility in *Drosophila* zydeco mutants 24-25

Virapat Kieuvongngam, Troy J.
Littleton, Yao Zhang

Reports

In search of the small cosmological constant

Joshua Millings, Sung C. S. Wong,
Yoske Sumitomo, Sze-Hoi H. Tye,
Edmund Bertschinger

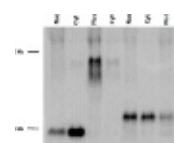


Recent experimental evidence indicates that a small cosmological constant is preferred in the Einstein Field Equation. Currently, theorists are experimenting with coupling scalar fields to gravity to explain the existence of the constant. Results presented here indicate that perturbations to quadratic potentials reduce the likelihood of the probability distribution peaking at zero.

27-31

1 kb regions of MALAT1 and NEAT1 are sufficient for RNA nuclear retention

Laura Y. Lu, Jeremy E. Wilusz,
Phillip A. Sharp

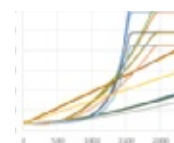


MALAT1 and NEAT1 are long noncoding RNAs that, when misregulated, have been implicated in a variety of human diseases including metastatic cancer and HIV. Little is known about the functions of these RNAs, but recent studies show that they localize to specific structures within the nucleus. In the current study, we aimed to identify sequence elements within MALAT1 and NEAT1 that are sufficient to cause a reporter mRNA to be retained in the nucleus.

32-41

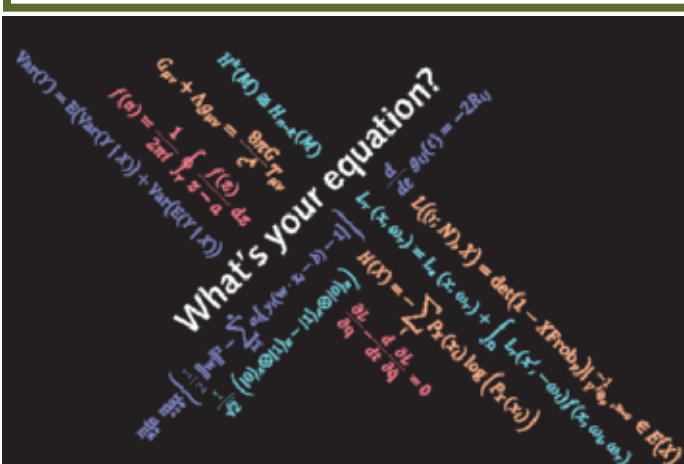
Salinity and density in deep boreholes

William DeMaio, Ethan Bates



In deep borehole nuclear waste disposal, waste canisters are exposed to high temperatures, pressures, and salinities. Canisters eventually compromise and soluble contents dissolve into the surrounding water. Subsequently, the decay heat could drive vertical convective flows and transport of radionuclides to the surface and humans. Based on an extensive literature search, various curve fits for salinity vs. depth are developed paper and a number of density vs. salinity relationships are reviewed.

42-48



Independent variables welcome.

The D. E. Shaw group is an investment and technology development firm with an international reputation and a decidedly different approach to doing business.

Combining insights from quantitative fields, software development, and finance, we're widely recognized as a pioneer in computational finance. And yet our culture doesn't fit the typical corporate mold: though we're competitive people, we're not competitive with each other.

The firm is currently looking for quantitative analysts, software developers, traders, information technologists, finance associates, and rotational associates.

Realize your potential. www.deshaw.com

DE Shaw & Co

Iain Cheeseman
MIT Associate Professor
Department of Biology
Member, Whitehead Institute



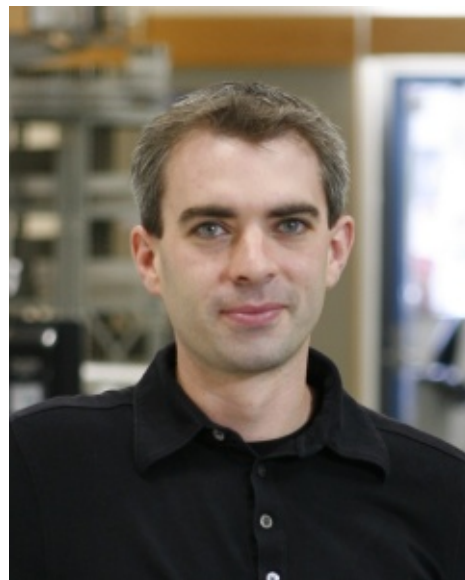
Massachusetts Institute of Technology
77 Massachusetts Avenue
Cambridge, Massachusetts 02139-4307
icheese@wi.mit.edu

December 2013

Dear MIT Community –

It gives me great pleasure to introduce this issue of the MIT Undergraduate Research Journal (MURJ). As a relative newcomer to MIT, I have been struck and impressed by the intellectual prowess and scientific passion of the undergraduates at MIT. It is wonderful to have this forum to highlight the work that undergraduates are conducting in the laboratories across MIT.

The percentage of MIT students who are actively participating in research projects through the Undergraduate Research Opportunity Program (UROP) is staggering. It is a big commitment to add working in a laboratory to the heavy course load at MIT. So why are so many MIT students adding research to their already busy schedules? I think that the simple explanation is because it's awesome. By design, most courses must focus on what is already known in a subject or a discipline. However, the most exciting part of science will always be the unknown. Although the pace of scientific progress is incredibly rapid, there is an amazing amount to still to be discovered.



The ability to identify an unanswered question, and then develop the ideas and approaches required to answer that question is by far the most satisfying part of science. I have always enjoyed reading the classic papers that provide the basis for textbook knowledge, but it is even more gratifying to tinker away in the lab on the questions that I am the most excited about. It is a profoundly motivating and exhilarating feeling to be the first person in the world to see a given result, no matter how small. It is this genuine scientific curiosity that is a hallmark of MIT, across the student body and the faculty.

The UROP is the ideal example of the MIT motto “Mens et manus” (mind AND hand) put into practice. The theory and facts that one learns in class need to be combined with the hands on experience of doing science. The UROP experience also allows one to see first hand that the

Iain Cheeseman
MIT Associate Professor
Department of Biology
Member, Whitehead Institute



Massachusetts Institute of Technology
77 Massachusetts Avenue
Cambridge, Massachusetts 02139-4307
icheese@wi.mit.edu

clean theory and facts from the classroom can be messier or contentious in the reality of science, and to learn how to do science in the most impressive research environment that I have ever experienced. The work conducted through UROPs contributes to the important research mission of MIT, and is the purest type of educational experience that anyone interested in science can have.

Sincerely,

A handwritten signature in cursive script that reads "Iain Cheeseman".

Iain M. Cheeseman
Cabot Career Development Associate Professor of Biology
Member, Whitehead Institute



**UNDERGRADUATE
RESEARCH JOURNAL**
Volume 26, Fall 2013

Editors-In-Chief

Ebaa Al-Obeidi
Sarine Shahmirian

Layout Chiefs

Cynthia Chen
Tatyana Gubin

Research Editor

Elliot Akama-Garren

Features Editor

Reuben Saunders

News Editors

Cher Huang
Linda Jiang

Copy Editors

Felicia Hsu
Amanda Liu
Lakshmi Subbaraj

Features Contributing Staff

Riley Drake
Anisha Gururaj
Felicia Hsu
Semon Rezhnikov

News Contributing Staff

Elliot Akama-Garren
Shahrin Islam
Skanda Koppula
Amanda Liu
Ruth Park
Danielle Penny
Lakshmi Subbaraj

Research Staff

Mahmoud Ghulman
Tatyana Gubin
Vania Lee
Amanda Liu

Treasurer

Reuben Saunders

Interdepartmental Liaison

Michael Yan

Production Advisor

Publishing Services Bureau

Printed at DS Graphics

MURJ Staff
MIT Undergraduate Research
Journal



**Massachusetts Institute
of Technology**
murj.mit.edu

December 2013

Dear MIT community,

We are thrilled to present to you the 26th issue of the MIT Undergraduate Research Journal. It has been a pleasure to work alongside hard-working staff to be able to present this issue to you today. The outstanding work of the undergraduate researchers in this issue is evident in their numerous findings that will no doubt make a positive impact on the MIT community and the scientific community at large.

The feature articles in this issue include “The World through the Eyes of a Trauma Surgeon” and our traditional Nobel spotlight, both written by outstanding MURJ staff. Research presented in this issue ranges from considering RNA nuclear retention to searching for the small cosmological constant in the Einstein Field Equation.

We would like to thank all of the student researchers, authors and editors for their tireless work on this issue and hope you enjoy it.

Best,

Ebaa Al-Obeidi
(Co-Editor-in-Chief)

Sarine Shahmirian
(Co-Editor-in-Chief)

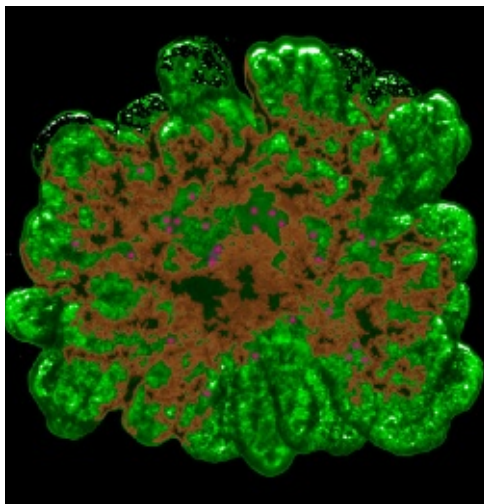
No material appearing in this publication may be reproduced without written permission of the publisher. The opinions expressed in this magazine are those of the contributors and are not necessarily shared by the editors. All editorial rights are reserved.

Science News In Review

MEDICINE

Miniature Pancreas Grown in Gel

The pancreas has many functions, including the production of enzymes and hormones essential in the digestion of food and the transfer of energy extracted from food to the cells of our bodies. Malfunction of the pancreas often results in a slew of problems, which can be counteracted by a transplant. However, pancreas donations are rare because, generally, they are only obtained from deceased donors.



Miniature pancreas grown in gel, in a picturesque tree-like structure.

Credit: <http://images.sciencedaily.com/2013/10/131015123527.jpg>

Researchers have been studying ways to artificially develop pancreases. Recently, an innovative 3-D method to grow miniature pancreases from progenitor cells was discovered by a lab at the University of Copenhagen.

This 3-D culture method enables efficient expansion of pancreatic cells, allowing cell material from mice to grow freely in tree-like structures. This method offers

huge long-term potential in producing miniature human pancreases from human stem cells. They would be valuable as models to test new drugs quickly and effectively without the use of animal models. In addition, they may be used as transplants with less probability of rejection by the recipient's body and higher rates of success because the pancreases could be specifically grown for each patient.

—R. Park

Source: <http://www.sciencedaily.com/releases/2013/10/131015123527.htm>

miRNAs Linked to Cancer Metastasis to Bones

Cancers can metastasize to bone, leading to overly active osteoclasts, cells that break down bones. A Princeton University study has recently identified miRNAs that can serve as potential biomarkers of this process, and that can even potentially be harnessed as therapeutics. miRNAs, or micro RNAs, are short sequences of RNA that can suppress the translation of specific genes.

In this study, changes in the levels of certain miRNAs were shown to correlate with bone metastasis, which occurs in 70% of cancer patients. Bone metastasis poses a serious threat to cancer patients because overly active osteoclasts are capable of creating bone lesions, fractures, and nerve compression. The fact the miRNA levels change with bone metastasis suggests that a change in protein expression takes place. In fact, two miRNAs that inhibit osteoclast genes (miR-141 and

miR-219) were found to be down-regulated in osteoclasts exposed to medium from cancer cells. When researchers then injected these miRNAs into mice that had transplanted cancer cells, they observed a decrease in the number of bone metastasis. David Waning, Khalid Mohammad and Theresa Guise of Indiana University in Indianapolis commented, “[miRNAs] could lead to improvements in diagnosis, treatment and prevention of bone metastases.”

—E. Akama-Garren

Source: <http://www.sciencedirect.com/science/article/pii/S1535610813004182>

New Drug Target for Cancer Treatment

Years of drug therapy research have produced only a limited number of targeted cancer treatments with the most commonly used therapies involving administration of high doses of intense radiation and toxic chemicals. These techniques, while effective in slowing and suppressing tumor growth, also cause damage to normal tissue. Recent research has been focused on discovering new drug targets that will avoid extensive normal tissue damage.

A potential new strategy to identify new drug targets for cancer treatment has been discovered by Professor Chad Myers, a computer science and engineering associate professor at the University of Minnesota's College of Science and Engineering, and Dr. Dennis Wigle, a thoracic surgical oncologist at Mayo Clinic. Meyers and collaborators used yeast genes to discover susceptible genes in cancer cells using synthetic lethal interactions. These interactions involve pairs of genes in which mutation in one gene alone causes no damage to

MATERIALS SCIENCE

Bending the World's Thinnest Glass

Just before glass shatters, its molecules bend, re-arrange, and melt. Because glass is an amorphous solid, with molecules not arranged in a definite lattice pattern, this deformation has been difficult to study.

Recently, researchers have been able to gain new insights into exactly what was happening by using a transmission electron microscope to image a new, world-record-setting, one-molecule-thick glass. With the electron microscope, scientists shot a beam of high-energy electrons at the glass, while also simultaneously imaging the resulting structural deformations.

They were able to observe the re-arrangement of atoms within the glass and found parts of the glass that were melted by the electron beam, thus, forming dynamic boundaries between glass's solid and liquid states. The ultra-thin glass allowed researchers to observe how glass breaks, atom by atom. There are numerous theories about the behavior of atoms within breaking glass, and



Shattering wine glasses.

<http://www.btnet.com.tr/wp-content/uploads/2012/11/glass.jpg>

many computer simulations of the process have been made. This ground-breaking study finally provides experimental evidence to lay some questions to rest. This knowledge can eventually lead to improved, atom-by-atom designs of products like window panes and transistors.

—L. Jiang

Sources: <http://www.sciencedaily.com/releases/2013/10/131015095638.htm>

the cell, but mutations in both genes cause cell death. Research in yeast genes to find synthetic lethality led to discovery of some homologous human genes that are frequently mutated in specific cancers.

By using this strategy, Myers and his team are enthusiastic that they will be able to discover many genes that are commonly mutated in cancer by searching through gene and public databases. What makes this research so exciting is that by using synthetic lethal interactions to identify drug targets, we have an alternative method of discovering different drug targets that won't necessarily harm normal cells. These drugs

could effectively kill cancer cells, while sparing other identical cells that lack the cancer-related genetic alteration identified through synthetic lethal interactions. Dr. Wigle notes that this strategy would be useful "particularly, for 'undruggable' cancer genes."

With this technology, Professor Myers, Dr. Wigle, and others are hopeful that better drug targets for cancer treatment can be found, providing a breakthrough in a personalized medicine approach to cancer treatment.

—L. Subbaraj

Source: <http://www.sciencedaily.com/releases/2013/10/131015113913.htm>

TECHNOLOGY

Finding Touch: Modern Prosthetics Research

Exciting research by scientists at the University of Chicago could play a pivotal role in the field of prosthetics. Through neurological experiments on monkeys, who have similar neural pathways as humans, researchers have been able to gain new insight on the sense of touch - and how to simulate it in a prosthetic device.

The study is a part of Revolutionizing Prosthetics, an interdisciplinary project which aims to restore touch and motor control in amputees via prosthetics technology. At the University of Chicago, a team led by Sliman Bensmaia, PhD, assistant professor in the Department of Organismal Biology & Anatomy, focused on researching sensory inputs.

First, the team researched the mechanisms behind contact location—that is, the sensation felt by where the skin has been touched. They found that when they electrically stimulated certain areas of the brain that corresponded to sensory inputs to fingers, their experimental subjects, monkeys, responded to the stimulus in the same way that they did to physical contact to their fingers.

The researchers also studied the sensation of pressure. They designed a system that applied specified amounts of electrical stimulation to the monkeys' brains - just like in the previous experiment, the animals' reaction to the artificial stimuli was the same as their response to the physical pressure.

Finally, the team experimented with contact events, which are characterized by bursts of activity after



Ground-breaking research at University Chicago could introduce touch technology to modern prosthetics.

Credit: <http://images.sciencedaily.com/2013/10/131014155638.jpg>

the hand first touches or releases an object. Once again, the experimental data showed that electrical stimulation could produce the same results as physical stimulation in monkeys.

Altogether, these results indicate how sensory information might be incorporated into a prosthetic arm via algorithms that control electrical stimulation to the brain. Such technology could be a significant advance in prosthetics technology, moving us one step closer to truly restoring touch.

—A. Liu

Sources: <http://www.sciencedaily.com/releases/2013/10/131014155638.htm>

NEUROSCIENCE

Glial Scarring Prevents Further Damage Following Spinal Cord Injury

Following injury of the central nervous system, stem cell-derived astrocytes develop a scar, the function of which has remained unclear. A study from the Karolinska Institute in Sweden demonstrates that this scarring is necessary to prevent worsening of lesions and neuron loss. Spinal cord injuries often result in irreversible paraly-

sis because nerve fibers are not able to regenerate, a limitation that has traditionally been attributed to glial scarring. Previously, glial scars were thought to inhibit regeneration by physically blocking axonal regrowth. However, when researchers in this study impaired scar formation by using

mice lacking neural stem cells, the spinal cord lesion expanded and more neurons died. Neural stem cells were also found to be essential for the production of neurotrophic factors, or chemicals that promote neuronal survival following spinal cord injury. These findings suggest that the previously held belief that preventing glial scar formation promotes recovery from spinal cord injury might actually do more harm than good.

—E. Akama-Garren

Source: <http://www.sciencemag.org/content/342/6158/637.full>

A New Perspective on Mind Reading

Recent studies by researchers at the Stanford University School of Medicine have led to discoveries that could contribute to mind-reading technology. Through monitoring the brain activity of study volunteers, researchers pinpointed a location in the brain - the intraparietal sulcus - that is devoted to quantitative thinking.

Such research on the correlation between thought and specific brain regions could lead mind-reading applications, though not in the dystopic setting that one might think.

Mind-reading could have medical purposes, including allowing a mute person to communicate to others by reading the patterns of activity in his or her brain.

Josef Parvizi, MD, PhD, the senior author of this study, and his team used a method called intracranial recording to study localized activity in the brain. The three volunteers of the study were patients with epilepsy, each with electrodes placed in the brain to monitor electrical activity, which reaches unnatural levels during an epileptic seizure.

Since the patients were monitored in an everyday hospital setting, the environment for the study mirrored that of real-life. Researchers asked patients questions that involved tapping into different cognitive abilities. Whenever the patients were asked a mathematical question, the electrodes read a spike of activity in the intraparietal sulcus. Moreover, the daily electrode records of the patients revealed that whenever there was increased activity in the intraparietal sulcus, the patient in question was doing something quantitative. This trend occurred even in the event of basic quantitative reasoning, such as the mention of “some more,” “many” or “more than.”



An MRI machine, which previous studies used to monitor activity in the intraparietal sulcus

Credit: <http://upload.wikimedia.org/wikipedia/commons/ee/MRI-Philips.JPG>

While the study gives new insight on a specific region of the brain devoted to quantitative reasoning, there's still a long way to go before an advanced mind-reading technology can be established. "We're still in early days with this," Parvizi said. "If this is a baseball game, we're not even in the first inning. We just got the ticket to enter the stadium."

—A. Liu

Source: <http://www.sciencedaily.com/releases/2013/10/131015123525.htm>

ECOLOGY

Researchers Link Climate Change to Pest Proliferation in North American Forests

As the MIT divest movement reaches full swing, startling evidence of the of climate change's real ramifications has slowly come to light...

Researchers from Dartmouth recently re-analyzed the ecological impact of climate change on biodiversity in North American forests – specifically, on the abundance of insects and other pests. The meta-study examined papers dating back to the 1950's as a way to rigorously observe changes to the forest equilibrium in the last-half century. Primary researcher Aaron Weed and his team found that the distribution and abundance of forest insects and other pathogens 'respond rapidly to climatic variation'. In particular, the average global temperature increase of 1 °F has increased the spread and reproductive capacity of many pestilent insects, often to much higher degrees than expected.

For example, the population of southern pine bark beetle has exploded – threatening forests that were previously protected by winter chills. Professor Matt Ayres, a researcher on Weed's team, suggests that the beetle may be 'the large-



Decaying trees in an area affected by the southern pine bark beetle.

Credit: <http://now.dartmouth.edu/2012/11/northern-forests-are-threatened-by-the-southern-pine-beetle/>

est source of disturbance in [North American] coniferous forests'.

The team hopes that their study will lay the groundwork for a more generalized theory that will help the nation cope with unprecedented climatic changes.

Until then, turn off a light and save a tree.

—S. Koppula

Sources: <http://www.sciencedaily.com/releases/2013/10/131015103953.htm>

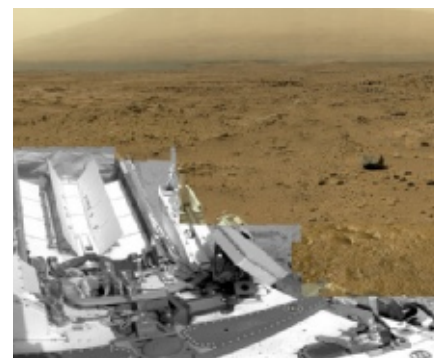
PLANETARY SCIENCE

According to Curiosity, Life on Mars Unlikely

After over a year on Mars, Curiosity is now yielding results that suggest life on Mars is unlikely. In a study conducted by the MSL Science Team, recently published in Science, researchers were unable to find sufficient enough levels of methane to give hope of life.

These scientists' interest in methane stems from both the fact that 90-95% of our atmospheric methane is biologically produced, and that in 2003, "plumes" of methane

were reported, at up to ten parts per billion by volume (ppbv).



A photo taken by Curiosity showing the Gale Crater near Mars' equator.

Credit: <http://graphics8.nytimes.com/images/2013/09/20/us/JP-MARS-1/JP-MARS-1-popup.jpg>

However, recent measurements produced a mean of only 0.11 ppbv--not nearly high enough to suggest life. Even these low levels could have come from Earth or meteors. Because neither the plumes nor the sudden drop in methane levels can be explained, scientists hope to continue the search for life, by perhaps finding alternative substances to look for, or by finding more encouraging results.

—D. Penny

Source: <http://www.nytimes.com/2013/09/20/science/space/mars-rover-comes-up-empty-in-search-for-methane.html?ref=space>

COGNITIVE SCIENCE

Cognitive Abilities of Rural Versus Urban Children

There have been many studies on the effect of the environment on cognitive development in children. It has already long been established that there is a disparity between the cognitive growth of high- and low-income children, but recently there has been a more detailed study on the differences in cognitive development among low-income children growing up in different environments. Dartmouth researchers have found that children raised in rural poverty areas scored significantly lower on visual working memory tests and slightly better on verbal working memory tests than children raised in urban poverty areas.

Working memory is the ability to hold multiple pieces of transitory information in the mind and manipulate them to complete a task or solve a problem. Studies have shown much stronger correlation

between working memory strength and academic success in comparison with IQ and academic success. One explanation for this phenomenon is that working memory is crucial to learning, from reading to math to decision-making.

One theory that explains the differences in cognitive growth between low-income urban and rural children points towards the minor differences in their daily lives within the environments in question. For example, studies have shown that chronic noise pollution is detrimental to verbal working memory, and rural areas generally have less noise pollution than urban areas. Urban



Juxtaposition of the different environments in question.

Credit: <http://cdn.theatlanticcities.com/img/upload/2012/04/06/crop3/largest.jpg>

areas also have many visual stimuli such as traffic, crowds, and signs, which are not as prevalent in rural areas. This may give rural children less opportunity to develop their visual working memory.

—R. Park

Source: <http://www.sciencedaily.com/releases/2013/10/131015123838.htm>

**A Tradition of Excellence**

Cornerstone Professional Park Suite D-101 43 Sherman Hill Road, Woodbury, CT 06798

T 203-266-0778/F 203-266-4759/info@civil1.com

<http://civil1.com>

MURJ Features

“We Do What We Do”: The World Through the Eyes of a Trauma Surgeon

When Michael Yaffe heard about the explosions at the Boston marathon, he rushed to the ER at the Beth Israel Deaconess Medical Center. Yaffe, a trauma surgeon as well as a Professor of Biology and Biomedical Engineering at MIT, spent the next 22 hours operating on blast victims.

BY ANISHA GURURAJ

Candles sit at the base of a small tree with white paper cranes hanging from its branches. Hundreds of running shoes hang from the gates next to countless bouquets of flowers. An array of Boston Red Sox hats occupies the corner. Next to them, a girl kneels on the ground with a permanent marker and writes “Boston Strong” on a square tile. A few yards in front of her, a board leaning against a tree trunk pictures an eight-year-old boy and the words “NO MORE HURTING PEOPLE. PEACE.” Signs nearby read, “Nashville believes in Boston,” and “Istanbul stands with Boston.” In the middle of it all, four white crosses — each with a vivid heart and printed names, Sean Collier, Lu Lingzi, Krystle Campbell, and Martin Richard — stand surrounded in a sea of stuffed animals, cards, and Bibles.

Outside this space, people bike, jog, or walk their dogs past the Boston Public Library, as they would on a normal Saturday morning. But only a sense of overwhelming sadness pervades the intersection of Copley Square and Boylston Street, where the memorial to the Boston Marathon bombing victims is full of quiet people with teary eyes, nearly a month after the bombings. Further down on Boylston, the



A memorial to the Boston Marathon bombing victims

bright yellow finish line of the marathon has been preserved; scattered groups of tourists speak in hushed tones about brothers Dzhokhar and Tamerlan Tsarnaev, who planted two bombs there on April 15. As the city recovers from the disaster which killed three people and injured over 260 others, donations continue to pour in for the victims while news outlets favor discussions about the prosecution

of the suspects. But the credit for restoring the strength of this city belongs also to another group of people who play an essential and often invisible role, not just in the aftermath of these events but also every seemingly ordinary day: the trauma surgeons of Boston's world-renowned medical centers.

This includes Dr. Michael Yaffe, a professor of biology and biological engineering at MIT and a trauma

surgeon at Beth Israel Deaconess Medical Center, who, at 2:40 p.m. on Monday, April 15, was at the YMCA, having just finished with the exercise bicycle where he had been working out the ankle he had broken several weeks before. At 2:45 p.m., he headed to the locker rooms and began packing his things to go home. As he was about to leave, the TVs in the locker room suddenly flashed “Breaking News”; there had been an explosion less than a hundred feet from the finish line of the marathon. “Nobody knew what was going on,” said Yaffe.

“I could just see that there were some injured people.” Ten seconds later a second bomb went off, 550 feet away from the first. He took out his phone to text one of his partners at the hospital, informing him that he had just heard about the blast and figured there might be some injuries: I’m not sure if we’ll get anything. Doubt it’s a mass casualty, but let me know if you need anything. His partner acknowledged the text with a “Thanks.” Six minutes later, Yaffe got a response: come in.

Beth Israel is one of five Level I trauma centers in the Boston area along with Mass General Hospital (MGH), Boston Medical Center (BMC), Brigham Women’s Hospital (BWH), and Tufts Medical Center. A Level I trauma center is a hospital equipped with the ability to provide the highest



Dr. Michael Yaffe, a professor of biology and biological engineering at MIT and a trauma surgeon at Beth Israel Deaconess Medical Center

level of emergency medical care to individuals with traumatic injuries. The Boston Metro area is also home to three pediatric Level I trauma centers, and numerous other hospitals, resulting in not only one of the highest-ranked medical communities, but also the highest density of trauma centers and trauma surgeons in the world. In fact, many experts, including some of the doctors who work at these hospitals, have argued in the past that the sheer number of trauma systems and medical facilities in the Boston area is simply a waste of resources and money.

No one was complaining now.

By the time Yaffe arrived at the hospital twenty-five minutes after the second bomb, about half the total patients Beth Israel would eventually receive from the bombings had already arrived. This included the most severely injured, such as those whose legs had been severed by the bombs. Yet, most of these initial patients had already been preliminarily treated—with some form of a

"In fact, many experts...have argued in the past that the sheer number of trauma systems and medical facilities in the Boston area is simply a waste of resources and money. No one is complaining now."

tourniquet, dressed wounds, and clamped exposed arteries—and they were rolled straight into surgery. This incredible efficiency and orderliness would continue for days after the initial bombing, to the point that the entire world would soon watch Boston and its medical centers manage to save every person who had entered hospitals with vital signs.

It is easy to overlook the significance of Boston's medical environment if you are not already an active member of that community. Despite the fact that Yaffe was my biochemistry professor at MIT and I have been conducting a research project under him for the past few months, I knew nothing about his work as a trauma surgeon, until Yaffe's secretary told me that he could not meet with me on April 16 because he had been operating for the past twenty-two hours straight on blast victims.

The system that trauma surgeons like Yaffe are part of is significantly more complex than at first glance. Dr. Paul Biddinger, the Director for Emergency Preparedness at MGH and Chairman of the Massachusetts Medical Society's Committee on Preparedness, defined a "trauma system" as a trained group of emergency physicians and surgeons and all of the supporting elements, such as anesthesiology, surgical subspecialties, and ICU care capabilities. The system emphasizes a continuum across the trauma spectrum, said Biddinger in an interview following the bombing. From the point of injury to the individual's recovery, which intersects everything from EMS (Emergency Medical Services) to rehabilitation centers, the goal is to ensure the utmost continuity of the entire range of possibility for medical care.

In Boston, the trauma response started on the ground, which Yaffe said made a huge difference. The

bombings themselves happened in the vicinity of the medical tent, so that there were a number of physicians already there prepared to treat runners, many of them with medical tourniquets. As he explained the significance of tourniquets to me in his office later, he reached into his bag, saying, "Being a trauma surgeon, I always carry one. You can never be sorry you had a tourniquet." He took out a circular strap from his bag and proceeded to show me how to tie it around his leg. "You tighten it further until you block the blood flow, and then lock it. And then you mark the time you put on the tourniquet and the letter T on the person's head to tell rescuers they have it on." Yaffe estimated that about 20% of the people who ultimately required tourniquets arrived at the hospital with medical tourniquets already in place; most others had temporary tourniquets fashioned out of belts, shoelaces or t-shirts. Over the years, tourniquets have gone in and out of medical fashion — at one point, they were thought to further aggravate injuries. In this case, they ended up saving many people from bleeding to death by the time they had reached the hospital.

When Yaffe arrived at the ER on Monday afternoon, action plans at all of the region's trauma centers were already being implemented. The foundation of this kind of plan started outside the front door, beginning with access control and security, so that people, particularly the walking wounded, would not be able to simply flood the hospitals. "The worst possible thing is for fifty people to be in the hospital waiting room with little cuts and injuries when there are people with legs blown off who need care first," said Dr. David King, a trauma surgeon at MGH.

The second and perhaps most important aspect of a mass casualty

response is triage, a process used in all medical emergencies to determine the order of priority in patients' injuries. But according to Yaffe, triaging for mass casualties is based on an entirely different set of principles than for regular civilian emergencies. "When you go to the ER, the first place you go is triage," he said. "There's a triage nurse there who asks you what's wrong. Her job is then to take the most severely injured people and treat them first. This is not what you do in a mass casualty, and not everyone understands that."

This makes perfect sense. In the civilian world, surgeons treat the most severely injured first because resources are infinite, and they can save the people who need the most help. But in a terrorist attack, gas pipeline explosion, or shooting, doctors and their supplies and operating rooms are limited. Instead, doctors treat those people who have the highest likelihood of survival with treatment but not without it. "So the walking wounded, people with broken arms, or ball bearings and shrapnel in their hand, you put aside," said Yaffe. "If you don't treat them right away they won't die." But the same goes for the people who are potentially too sick or hurt for you to help. "If you see brain protruding and oozing out of the skull, forget it, don't waste your time. If you see a horrendous torso injury, like the lung is gone and you're seeing the heart, you probably can't do a whole lot of good. But if the patient's abdomen is expanding in front of you, and they're talking, those are the people you want to take to the OR because it's probably a spleen injury. Use your resources to save people like the guy whose legs got blown off who will die if I don't treat him, but if I do, he has a high likelihood of survival."

Luckily for the hospitals, the EMS on the ground had triaged exceptionally well on the scene itself. "It's really easy to see a man with a broken hand and immediately stick him into an ambulance and send him off to the hospital," said King. "It's much more difficult to tell him to wait because there are two people behind him both with their legs blown off who are bleeding to death and need to go in first." The fast decisions EMS made on the ground were a result of practice, preparation and their understanding of the needs of the rest of the trauma system. Back at MGH, trauma surgeon Dr. Peter Fagenholz, who had just finished an operation in the ICU and was the first surgeon in the ER after the initial alert, said that the five most critical patients were the first five in, in almost perfect order of acuity. Later, he saw on the news that all of the hospitals had received similar numbers of patients, meaning that no one hospital had been swamped

"Calmness and objectivity are paramount because you're responsible for the best possible outcome, for your patients. Losing objectivity will hinder you in that job."

by incoming patients. "It seems to me like that triage is harder than what we had to do, and it was really done very well," he said.

Elaborate plans involving these elements (access control, triage and so on) have been conceptualized by Boston hospitals in regular drills ever since 9/11. The Marathon bombings, however, served as the first test for whether these plans would actually work effectively in reality, and the system passed with flying colors. Both King and Yaffe said that the responses in their hospitals worked better than any tabletop exercise they had ever done, and brought out the best in these professionals, many of whom

were not in the best condition to be performing treatments of this magnitude. King himself, for example, had just crossed the finish line as a runner in the Boston Marathon, fifty-seven minutes before the first bomb. On his cab ride back home with his family, his phone suddenly buzzed with a text message about the explosion; he barely had time to drop off his family before returning to the hospital and conducting twenty hours of surgery, despite immense physical exhaustion.

Trauma surgeons are part of a clear structure of responsibility in an environment of chaos. Yaffe described a head trauma surgeon

overlooking the process at Beth Israel while another trauma surgeon took charge on the floor of the ER. This kind of organization allowed for the best care to reach the patients, so that when a patient arrived with horrendous burns, he was immediately placed in front of Yaffe, who is a burns specialist, and one of the few there who could have tended properly to him.

Trauma surgeons like Yaffe, King, and Fagenholz encompass almost the entire range of the medical



An example of a trauma surgery team operating in the U.S. Marine Corps

spectrum. At the most basic level, they recognize patients who can benefit from immediate surgical attention. But ultimately they can do everything including the definitive operative care, says

Dr. John Fildes, medical director of trauma for the American College of Surgeons. “There aren’t a lot of doctors who can carry a process up to the top like that.”

Because trauma encompasses such a wide range of medical possibilities, trauma surgery requires an entirely different attitude than general surgery. Yaffe was quick to say that while general surgery allows for plenty of time and is meant to reconstitute someone’s anatomy to its normal state, the purpose of trauma surgery for a mass casualty is quick damage control. When patients arrived who had lost so much blood that they had turned completely white, Yaffe could not focus on the broken hand or the shrapnel stuck in their arms. He had to immediately open up the abdomen, and look for and fix any obvious holes. With many of the patients whose legs were extremely disfigured, both time and resources dictated that he amputate them immediately, whereas in normal situations he might have gone to great lengths to save the leg. Then the patient was taken to the ICU to be resuscitated, and Yaffe moved on to the next patient. Twelve hours later, if the first patient had reached a stable condition, he would go back to fix the next level of injuries. “Our goal in the first surgery is extremity injuries, not to do a definitive operation,” he said. “You figure out what you can save and what you cannot save.”

The trauma surgeons I talked to across the board made it clear that horror and emotional shock that

"We just feel most comfortable and most relaxed in the presence of this incredible chaos,... I don't know what to say — we do what we do."

most of us experienced when we heard about the bombings were far from their minds when they were in the center of the action. Fildes says it’s part of the culture of training trauma surgeons. Calmness and objectivity are paramount because “you’re responsible for the best possible outcome, for your patients. Losing objectivity will hinder you in that job.” When I asked Fagenholz about how they prepared psychologically for operating in a situation like this, I was struck by his blunt acknowledgement of the similarity of treating the bomb blasts on a surgical level to what he experiences each day in his job. “Every day I see someone in the ER, I see someone in trauma who didn’t expect to be there who’s having something terrible happen to them. You have to explain it to them if they’re in a state to talk to you, or to their family if they’re not — we do that every single day.”

A few days after the bombing, Brigham Women’s Hospital surgeon Atul Gawande wrote a post for the New Yorker about the readiness of Boston hospitals for the tragedy, attributing much of the response’s success to the grim reality we have come to live in. Certainly, there’s a lot to be said for “post-9/11 sobriety.” Yet, the readiness of the hospitals belongs not simply to the institution of action plans or even society’s realistic attitude to such a tragedy, but also to the sheer talent, experience and grit of the Boston medical community — to these trauma surgeons who witness each day the gravest of human conditions. People like Yaffe and

King and Fagenholz, the supporting staff of nurses and technicians, and the EMS system become an integral core that we often unknowingly place our complete faith in, not only to be there when disaster strikes, but also to work to their maximum potential and restore the lives of the people we love.

Yaffe had no intention of being a trauma surgeon (he wanted to become a surgical oncologist), but he pursued his M.D./Ph.D. in Cleveland, where the county hospital was always teeming with trauma cases. “Cleveland was a knife and gun club,” he said. “In fact, we used to call morning rounds the ‘bullet club.’” After years of getting used to working for 36-48 hours straight and witnessing evening trauma rounds blending into mornings, Yaffe decided that he hated working in the trauma unit and would never do it again. Ultimately though, by the time he had finished his residency, he ended up having more trauma experience than any other resident and realized his talent in the area. “It’s an adrenaline rush,” he said. “You live for it. You totally live for it.”

Back in Yaffe’s office, a smile spreads across his face as he tells me how his sister, a trauma flight nurse, texted him after the bombing in utter jealousy that he would be working on the victims of the bombing. “We just feel most comfortable and most relaxed in the presence of this incredible chaos,” he says laughing. “I don’t know what to say — we do what we do.” ■

Nobel Spotlight: Professor Phillip Sharp MIT Department of Biology

This issue's Nobel Spotlight features Professor Phillip Sharp, 1993 Nobel Prize winner in Physiology or Medicine. Look for the second part of this interview in the next issue.

BY REUBEN SAUNDERS, RILEY DRAKE, & SEMON REZCHIKOV

MURJ: *You got your PhD in chemistry. Why did you decide to become a molecular biologist?*

Sharp: I started making the movement as I was getting my PhD from the University of Illinois. I had done my thesis on the hydrodynamics of polymers, particularly DNA, and toward the end of my graduate work I started to read the molecular biology literature at that time. I picked a Cold Spring Harbor Symposium, I think it was the 1967 volume, where then as now they bring the experts in the subject and summarize the worldwide knowledge in that subject in one of these books, and it was on genomes and chromosomes, and I looked at it and to me it was very clear that there were some really profound questions of great importance to be understood, where not even the faintest outline of the answers were clear. There were new physical techniques that were being developed at the time, including electron microscopy, DNA hybridization, and DNA fractionation, and these problems seemed approachable and possibly answerable. I was looking for things to commit myself to, and it seemed like this was one of those moments in which there were a set of important questions that

could be answered with newly emerging tools. It seemed it would be great fun to be a part of that.

At the time, center of gravity in molecular biology was in bacterial organisms, because they could be handled, because they could be grown, and because mutants could be made and very sophisticated science could be done. However, the questions that really fascinated me were about the more complicated human cell, the mammalian cell, and the mammalian organism. I wanted to go beyond just bacterial molecular biology, I wanted to be part of a smaller group of people that was interested in elucidating some of the fundamental aspects of mammalian molecular biology, particularly genes and how genes were regulated, so that took me into more new frontiers, even, into molecular and cell biology and led me to concentrate on viruses as a tool to actually study molecular biology in our mutant cells.

MURJ: *You spent some time at Cold Spring Harbor working with James Watson?*



Professor Phillip Sharp, 1993 Nobel Prize winner in Physiology or Medicine

Credit: <http://www.oligotheapeutics.org/ots/wp-content/uploads/2012/10/Keynote-Phillip-Sharp-PhD.jpg>

Sharp: After my postdoc, I spent some time looking for a job. It was pre-“War on Cancer” and federal funding for research was stagnant. It wasn’t a good time to look for new positions. I interviewed at a number of places and luckily I didn’t get an offer, because I would have felt compelled to go. James Watson was putting together a group to study DNA tumor viruses, and I wrote him and said I would like to learn how to grow and handle DNA tumor viruses, and he offered me a postdoctoral job. I went there



Phillip Sharp with his mentor, James Watson, in 1987.

Credit: Sharp Lab archives

for one year and then he made me a staff member and I stayed for 2 more years before I came to MIT. It was a very stimulating and productive environment—I must have published or been an author on 10 or 15 papers in those three years, and I learned an enormous amount. It's remained, since Jim has been leader of it over the last 30 or so years, it has grown and remained to be a very vibrant research institute out there on the North Shore of Long Island.

MURJ: You moved to MIT to work at the Cancer Research Center?

Sharp: Yes, in 1974, it had just been opened. Salvador Luria, who was a Professor here and the mentor of Jim Watson, there's an interesting story there, came to MIT in the late 50s and recruited, with others, a staff of very exciting young people and some very established figures. I don't want to mention all of their names, because I'd leave someone out and they

would be upset. He recruited Dave Baltimore and Dave Potstein and Harvey Lodish and a whole host of young people, but particularly Dave Baltimore, who was an emerging star in mammalian cell biology studying viruses. He started with Polio and then went to retroviruses and discovered Reverse Transcriptase, which turns RNA to DNA. I'd met David at meetings when I was at Cold Spring Harbor, and in fact even before, and I knew there would be a vibrant community around him. Luria and Baltimore applied to the National Cancer Institute for a basic science cancer center here, and they were awarded one, and they raised some money and renovated a building and built the center. I came in 1974 just as building was being occupied. I was on the same floor as David Baltimore and Bob Weinberg, who had been recruited at the same time, as well as Dave Housman and Nancy Hopkins. There were 5 of us on the floor in 1974-75. It was an extraordinarily active research community. All of those 5 are now

members of the national academy, so it was a good group and a good time to be together doing research. The cancer center ultimately had 5 Nobels associated with it: Luria got a Nobel, Dave Baltimore received a Nobel, Susumu Tonegawa, who had been recruited at the time, received a Nobel, I received a Nobel, and Bob Horwitz, who was here in the building but not a member of the cancer center also received the Nobel. The density of Nobels related to that institute was extraordinarily high.

MURJ: Today when we think of cancer, we think of a disease caused by a mutation in a cell's DNA that causes unregulated cell growth. When the Center for Cancer Research was first established, how did researchers understand cancer?

Sharp: It was conceived of from several aspects: Clearly it was a property of a cell, because you could isolate cells from tumors and they had different properties than cells from normal tissues. They would grow for longer periods of time, they would grow, displace from one another in suspension, they were clearly different. When we looked at the chromosomes of them, we knew there were chromosomal changes, mostly major, and we knew that there were copy number changes, but we didn't understand what that meant (we still don't), and we knew there were viruses that caused cancer. Rous early on showed that the Rous sarcoma virus created muscle tumors and we knew that viruses created warts. We knew there were some genes you could put in and cells and create tumors, and that's where the knowledge stood.

There was a very important experiment done by Varmus and Bishop where the Rous virus, when

people started studying it as a combined chemical genome, it was recognized from genetics and the physical science that there was a segment of the Rous virus that had nucleic acid that was critical for creating the tumor in the animal. You delete that, you don't get the tumor; you mutate that, you don't get the tumor. Varmus and Bishop showed that if you isolate that part of DNA, if you carried out hybridization across species, you could find those sequences in those species, suggesting that it was a cellular gene that had been captured by the virus and expressed by the virus created tumors.

That was the earliest data, but that it proved that there was a gene that created tumors in chickens, but it was in the cancer center that Bob Weinberg first isolated an oncogene from a human cell and that was Ras, the most commonly mutated oncogene in cancer, and that really was the sea change in

terms of the focus on mutations in somatic tissue that then contributed to the tumorigenicity itself. That really happened next door down the hall from where I was, and it was an absolutely remarkable advancement. All of a sudden we understood that cancer involved mutation, but we didn't know how many, and then we understood there could be two, Myc for proliferation and the other Ras for other properties, and then Weinberg showed that there could be cooperation between the two—it was a very exciting time. That was where the field stayed until genomics. Now we sequence the genome and know that there are hundreds of mutations in some cancers and none that we can find in others. In many childhood tumors we don't even know why these children are developing tumors because the genome is almost completely normal, but

that's a rarity, typically you find 10s to hundreds of mutations in cancer cells.

MURJ: How did you discover that RNA was spliced?

Sharp: Early on when I was a postdoc at Caltech, I listened to all the people around me who were studying development, how a single cell makes a multicellular organism, how cancer developed, how everything else developed. It seemed obvious to me that at the heart of all this there had to be changes in the expression of genes, and, puzzlingly, we didn't even know what a gene looked like in mammalian cells. It seemed like we were all babbling about all these things, but we hadn't really identified what we were talking about.

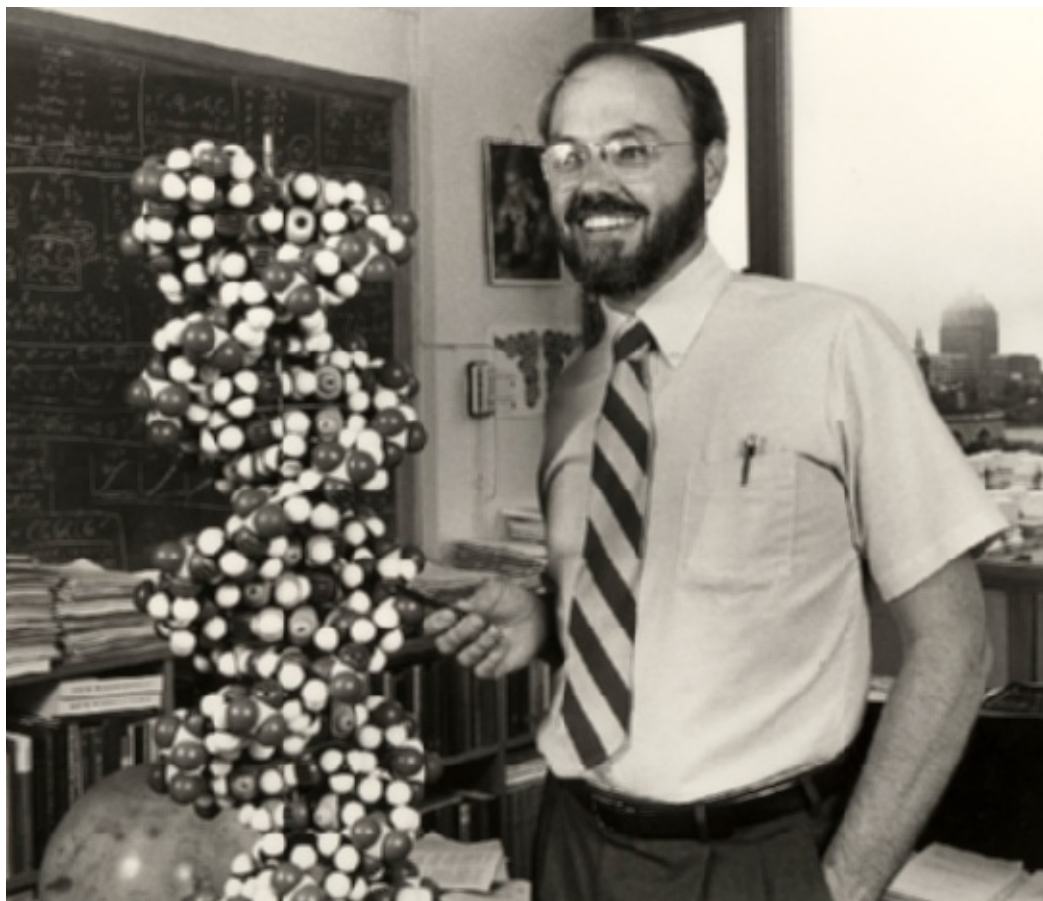
It seemed like a straightforward question to ask and answer, but very people were interested, which is why it hadn't been answered when I got there. People in bacterial molecular biology knew what a bacterial gene looked like: it was a piece of DNA that went from here to there. There were hints in molecular cell biology of mammalian cells that the genome was in much larger, it was in the nucleus, not the cytoplasm, and the most gene-proximal form of RNA seemed very large relative to the smaller size of messages in the cytoplasm.

Recombinant DNA hadn't happened yet, so we couldn't isolate DNA. Instead, I started introducing adenoviruses to cell and looking at viral DNA expression. My students Sue berget and Claire Moore and I started realizing that there was this discontinuous structure to a gene—exon, intron—in the fall of 1976, and by January '77 we were writing a paper saying "splicing." By the summer of '77, across the world, everybody understood this



The MIT Center for Cancer Research, freshly renovated in 1974.

Credit: Sharp Lab archives



Phillip Sharp in his Center for Cancer Research office, in the late 70s.

Credit: Sharp Lab archives

new gene structure existed, and it was being discovered in all sorts of cellular genes, and it was an incredibly exciting time.

I would say this to a student coming into research: “Never overlook the obvious, basic question because frequently, when you try to address that question with new technology and a deeper way, with more detail, you will discover things that are very interesting. It is always exciting to be out there on the forefront pitching into the unknown, but you can pitch into the unknown by being very detailed and looking at something you think you know in a much more fundamental way. That’s what happened that led us to the discovery of gene structure—we just looked more deeply.

MURJ: What sort of hints did you have?

Sharp: The real direct hint is that when you pulse label newly synthesized RNA, the RNA that you label in higher cells, when you put it only the only technology you have at that stage to measure its length, sedimentation [a way of determining the mass of a molecule], it sediments very fast. However, if you label for long periods of time, like the time of a cell division, 24 hours, then the major population of the RNA in a cell is gene-sized, 2000 nucleotides. There is this population of very rapidly sedimenting things in the nucleotide and slower-appearing gene-sized stuff in the cytoplasm. They were the same sequence: you could actually say “Those sequences will hybridize to the

same sequence as these do.” And then it gets a bit more ridiculous: there is poly-A on the 3’ end, both in the nucleus and in the cytoplasm. And there are 5’ caps, both in the nucleus and on the cytoplasmic message. You have caps on the 5’ end and poly-A on the 3’ end, but the nuclear RNA was 3 times to 10 times as large as the cytoplasmic RNA was. No one ever thought that you could cut stuff out of the middle. As soon as you look at the big picture, though, it was obvious that you were cutting stuff out of the middle. The reason you couldn’t cut things out of the middle was because that’s where the protein coding was—you couldn’t cut things out, that was too critical! You could lose your reading frame and you are out of it—but of course, that’s

the way it works.

If you go back and read that literature as a scholar, you just read it and wonder why everyone didn’t understand that this is what was happening—but as soon as we saw it in an adenovirus, it was accepted everywhere. One of the great crushing things that happened to me, I made a fundamental discovery that changes everything, the textbooks, everything we knows, and within 6 months it was old news. I could go anywhere and give a seminar and people would ask “What’s new?” I had been at MIT only 3 years and had a group of maybe 5 people. The biggest labs in world started working on the subject. It was fascinating, but also incredibly aggravating. ■

MURJ UROP **Summaries**

Bio-Inspired Strong-yet-Tough Polymer Composite Reinforced by Water

Samuel Lim¹, Mingming Ma², Robert Langer³

¹Student Contributor, Class of 2014, Department of Chemical Engineering, Massachusetts Institute of Technology (MIT), Cambridge, MA 02139, USA

²David H. Koch Institute for Integrative Cancer Research, MIT, Cambridge, MA 02139, USA.

³Harvard-MIT Division of Health Sciences and Technology, and Department of Chemical Engineering, MIT, Cambridge, MA 02139, USA.

Background

In designing most polymeric structural materials, strength and toughness are two of the most important qualities to consider. Although these two terms are often used interchangeably in everyday life, they in fact refer to very different mechanical properties; strength measures the resistance of a material to deformation, whereas toughness measures the energy required to cause fracture¹. Since structural material that is hard but ruptures very easily is undesirable, it is important to develop a strategy that can achieve good strength and toughness simultaneously.

Polypyrrole (PPy) has broad biomedical applications such as artificial muscle, biosensor and drug delivery, owing to its good conductivity, and high tensile strength². Yet, its poor toughness due to low stretchability limits its application to where flexibility is required³.

In this study, we report the synthesis of polyol borate – PPy composite film that has significantly improved toughness compared to that of conventional PPy film. The unique, bio-inspired design of this material makes it responsive to the environmental humidity⁴. Thus, we investigated the effect of humidity on the mechanical properties of the film, and then probed the mechanism by which the sorption and desorption of the water molecule regulate the film's properties.

Structure Design and Synthesis

Our polymer composite film has a combination structure of a rigid PPy matrix and an elastic polyol-borate network; this structure allows the film to be strong and flexible at the same time. The design was inspired by the animal dermis structure, in which a soft elastin microfibrils form network structure with rigid collagen fibers.

The synthesis was achieved through the electropolymerization of pyrrole on the platinum electrode, in the presence of polyol borate. Various polyols with different characters such as molecular weight, hydrophobicity and structural linearity were tested in order to determine which polyol yields the product with the best toughness and strength; pentaerythritol ethoxylate (PEE) was chosen as a result.

Mechanical Properties and Effect of Humidity

The composite film synthesized at relative humidity of 60% possessed significantly high toughness compared to the PPy film; tensile strength was similar to that of typical PPy film. Ambient humidity had a notable effect on the mechanical properties of the film. Compared to the film made at 60% humidity, it was slightly stronger but less tough under dry condition, whereas it was weaker and less tough under very humid condition. Thus, we concluded that 60% relative humidity was the best condition that yields the toughest polymer film with acceptable strength.

Mechanism of Humidity-Responsive Behavior

In order to explain above effects of humidity, we hypothesized that the network structure of the polymer composite film is maintained by the intermolecular hydrogen bond between PPy chain and polyol borate. In this case, the presence of environmental water molecules can disrupt the network, making the film water-responsive. Solid-state NMR analysis results supported our assumption; we observed rigid structure under dry condition, as opposed to “swollen” structure caused by water adsorption under humid condition. At moderate humidity, the structure was in the mixed state; this partially rigid and partially swollen structure is likely to be the reason why the film showed both good toughness and strength at 60% humidity.

Conclusion

In this study, we successfully synthesized the polyol borate – PPy polymer composite film, which is not only sturdy but also flexible. Moreover, we confirmed the mechanism by which environmental water molecules reinforce the film structure to further improve its mechanical characters. Our composite film’s bio-inspired

design, as well as its unique interaction with water, marks a novel strategy of achieving both good strength and toughness, which are often difficult to achieve simultaneously.

References

1. Ritchie, R.O. The Conflicts Between Strength and Toughness. *Nature Materials*. 10, 817-822 (2011).
2. Geetha, S., Rao, C.R.K., Vijayan, M., Trivedi, D.C. Biosensing and Drug Delivery by Polypyrrole. *Analytica Chimica Acta*. 568, 119-125 (2006).
3. Sasso, C., Zeno, E., Petit-Conil, M., Chaussy, D., Belgacem, M.N., Tapin-Lingua, T., Beneventi, D. Highly Conducting Polypyrrole/Cellulose Nanocomposite Films with Enhanced Mechanical Properties. *Macromolecular Materials and Engineering*. 295, 934-941 (2010).
4. Ma, M., Guo, L., Anderson, D.G., Langer, R. Bio-Inspired Polymer Composite Actuator and Generator Driven by Water Gradients. *Science*. 339, 186-189 (2013).

GENERAL DYNAMICS
 Electric Boat

Get your career underway





The Nuclear Submarine Has Long been the silent backbone of United States Naval Supremacy. **ELECTRIC BOAT** designs and builds these incredible machines.

We are looking for energetic and innovative individuals to continue the tradition of excellence that has become synonymous with **ELECTRIC BOAT**. We will show you how to apply your skills to the art of nuclear submarine design, engineering and construction.

ELECTRIC BOAT has immediate openings in Groton, Connecticut, for entry level engineers with zero to three years experience.

ELECTRIC BOAT is looking for engineering candidates with a minimum of a Bachelors degree in:

- Aerospace • Chemical • Civil • Computer
- Computer Science • Electrical • Mechanical
- Marine/Ocean • Naval Architecture

ELECTRIC BOAT offers an excellent salary and benefits package, including Tuition Reimbursement, Relocation assistance, and an excellent 401K Plan.

GENERAL DYNAMICS
 Electric Boat
 75 Eastern Point Road
 Groton, CT 06340-4969

Please visit www.gdeb.com/employment for more information, or contact Electric Boat Employment office at 1-888-231-9662

US Citizenship Required Equal Opportunity/Affirmative Action Employer

★
Institute for Defense Analyses
★

For over half a century, the Institute for Defense Analyses has been successfully pursuing its mission to bring analytic objectivity and understanding to complex issues of national security. IDA is a not-for-profit corporation that provides scientific, technical and analytical studies to the Office of the Secretary of Defense, the Joint Chiefs of Staff, the Unified Commands and Defense Agencies as well as to the President's Office of Science and Technology Policy.

To the right individual, IDA offers the opportunity to have a major impact on key national programs while working on fascinating technical issues.

broaden your perspective

your career • your future • your nation



IDA is seeking highly qualified individuals with PhD or MS degrees

Sciences & Math	Engineering	Other
<ul style="list-style-type: none"> • Astronomy • Atmospheric • Biology • Chemistry • Environmental • Physics • Pure & Applied Mathematics 	<ul style="list-style-type: none"> • Aeronautical • Astronautical • Biomedical • Chemical • Electrical • Materials • Mechanical • Systems 	<ul style="list-style-type: none"> • Bioinformatics • Computational Science • Computer Science • Economics • Information Technology • Operations Research • Statistics • Technology Policy

Along with competitive salaries, IDA provides excellent benefits including comprehensive health insurance, paid holidays, 3 week vacations and more – all in a professional and technically vibrant environment.

Applicants will be subject to a security investigation and must meet eligibility requirements for access to classified information. U.S. citizenship is required. IDA is proud to be an equal opportunity employer.

Please visit our website www.ida.org for more information on our opportunities.



Please submit applications to: <http://www.ida.org/careers.php>

Institute for Defense Analyses 4850 Mark Center Drive Alexandria, VA 22311

RNAi screen for suppression of epileptic seizure susceptibility in *Drosophila* zydeco mutants

Virapat Kieuvongngam¹, Troy J. Littleton², Yao Zhang³

¹Student Contributor, Class of 2015, Department of Biology, Massachusetts Institute of Technology (MIT), Cambridge, MA 02139, USA

²Department of Brain and Cognitive Science, MIT, Cambridge, MA 02139, USA.

³The Picower Institute of Learning and Memory, MIT, Cambridge, MA 02139, USA.

Introduction

Communication between neurons and glial cells has been shown to be important for the regulation of neural excitability. Dysfunction of glial-neuron communication pathway can contribute to pathological conditions. There is evidence that some cases of idiopathic epilepsy are results of dysregulation of neural excitability (Melom & Littleton, 2013).

A previous study by Jan Melom and Troy Littleton, showed that glial-specific Na⁺/Ca²⁺,K⁺ exchanger, zydeco (*zyd*) is essential for intracellular Ca²⁺ oscillation in cortex glia (Melom & Littleton, 2013). Zydeco mutant is found to have elevated intracellular Ca²⁺ level in cortex glia and to have increased susceptibility to seizures induced by environmental stimuli, such as high temperatures. This discovery implies the role of glial cells in regulating neuronal excitability.

Genetic screen

We investigated molecular regulators that are involved in glia-neuron communication. To determine which genes are responsible for this pathway, we performed behavioral screens for suppression of heat-induced seizure phenotype in *zyd* background. We used the UAS/Gal4 system to express shRNA hairpins specifically in glial cells. The suppression screen was set up as indicated in Figure 1.; F1 progenies from the cross were subjected to the behavioral test. We have identified a number of RNAi lines that can suppress temperature sensitive seizures in *zyd* mutants.

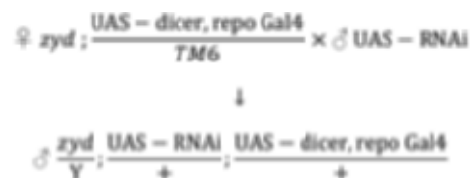


Figure 1. Genetic screen for suppression of heat-induced seizure.

Several hits from the suppression screen are found to be associated with endosome and lysosome maturation. Because the shRNA was specifically expressed in glial cells, the rescue from temperature sensitive phenotype suggests a role of endosomes or lysosomes in glial-neuronal communication (Chanut-Delalande et al., 2010). These genes include Hrs (hepatocyte growth factor receptor tyrosine kinase substrate), Stam (signal transducing adaptor molecule), SNAP-25 (synapse protein-25), and syx-13 (syntaxin-13).

Discussion

In fall of 2013, we focus on the result of the genetic screen, with particular emphasis on Hrs and Stam in regulating endosome and lysosome maturation. Two hypotheses will be empirically tested. One is that the disruption of endosome maturation rescues TS seizure phenotype because the RNAi disrupts the lysosomal exocytosis, which is responsible for modulating neuronal excitability. This hypothesis is supported by the evidence that glial lysosomes release neuromodulators, such as ATP or glutamate (Zhang et al., 2007).

There is evidence that Hrs and Stam function in initial selection of protein degradation or plasma membrane

localization (Chanut-Delalande et al., 2010). We develop a hypothesis that the disruption of endosome lysosome regulation may impair the plasma membrane localization of ion channels or receptors that counteract the effect of zyd, and therefore the proteins are involved in modulating neural excitability.

To elucidate the role of RNAi hits, including Hrs and Stam, we will perform experiments as described here.

1. To study the effect of candidate genes in neuronal excitability in general, we will perform a temperature sensitive behavioral assay of Hrs-RNAi or Stam-RNAi in wildtype background. We will also perform this assay in Hrs and Stam overexpression genotypes.
2. To investigate the effect of candidate genes in endosome and lysosome function, we will use imaging techniques to visualize endosome and lysosome markers in zyd or wildtype background.
3. To test whether Hrs or Stam is involved in the trafficking receptor or ion channel, which functions antagonistically to Zyd at the glial membrane, we will visualize the intracellular Ca²⁺ dynamics in Hrs-RNAi or Stam-RNAi in zyd background.

Conclusion and future directions


Our result suggests that the endosomal/lysosomal pathway may play a role in glia-neuron communication. We would like to characterize other components of this pathway, in particular the molecules being regulated by Hrs and Stam. We are also interested in exploring the role of the endosome/lysosome pathway in regulating the release of glia-derived neuromodulator. These experiments could help to gain more insight into the molecular mechanism of how glia regulate neural excitability.

References

1. Chanut-Delalande, H., Jung, A. C., Baer, M. M., Lin, L., Payre, F., & Affolter, M. The Hrs/Stam complex acts as a positive and negative regulator of RTK signaling during *Drosophila* development. 2010. *PLoS one*, 5(4), e10245.
2. Melom, J. E., & Littleton, J. T. (2013). Mutation of a NCKX eliminates glial microdomain calcium oscillations and enhances seizure susceptibility. *The Journal of neuroscience : the official journal of the Society for Neuroscience*. 2013. 33(3), 1169–78.
3. Zhang, Z., Chen, G., Zhou, W., Song, A., Xu, T., Luo, Q., ... Duan, S. (2007). Regulated ATP release from astrocytes through lysosome exocytosis. *Nature cell biology*. 2007. 9(8), 945–53.

Electrical Construction ♦ Fire Alarm ♦ Special Projects ♦ Tel-Data/Security Systems

**Proud to Help Build
A Bright Future
for MIT**



JMB
Since 1921

J & M. BROWN COMPANY, INC.
Excellence in electrical construction

SPECTRUM
Integrated Technologies

NECA
ANALYSIS SYSTEM

Jamaica Plain, MA Tel: 617.522.6800 www.jmbco.com

CALLING ALL INVENTIVE STUDENTS!

The Lemelson-MIT National Collegiate Student Prize Competition is open to students nationwide who have inventions in one of two categories:



"Cure it!"
(Healthcare)



"Use it!"
(Consumer devices
and tools)

\$15K to the winning individual graduate student in each category
\$10K to the winning undergraduate team in each category

Apply by: December 31, 2013

<http://mit.edu/invent/studentprize>

LEMELSON-MIT
Celebrating innovation, inspiring youth

MURJ Reports

In Search of the Small Cosmological Constant

Joshua Millings¹, Sung C. S. Wong², Yoske Sumitomo², Sze-Hoi H. Tye², Edmund Bertschinger³

¹Student Contributor, Class of 2016, Department of Physics, Massachusetts Institute of Technology (MIT), Cambridge, MA 02139, USA

²Institute of Advanced Study, The Hong Kong University of Science and Technology, Clear Water Bay, Kowloon, Hong Kong

³Department of Physics, Massachusetts Institute of Technology (MIT), Cambridge, MA 02139, USA

Recent experimental evidence indicates that a small cosmological constant is preferred in the Einstein Field Equation. Currently, theorists are experimenting with coupling scalar fields to gravity to explain the existence of the constant. This project will explore quadratic and cubic scalar fields, using their minima to represent the vacuum energy of the universe. Perturbations to quadratic fields will be explored to see their effect on the peaking behavior at zero-the approximate value of the cosmological constant. This project's result indicates that perturbations to quadratic potentials reduce the likelihood of the probability distribution peaking at zero. In the future, analytical approximations will be examined to gain a more complete understanding of the perturbations' effect on the probability distribution.

Introduction

Due to recent experimental information, the universe is thought to be expanding.^{1,2} This counter-intuitive result is believed to stem from the cosmological constant coupled to Einstein's Field Equation, explaining gravity effect on the universe. We postulate that the constant can be represented by a potential field and, for simplicity, we choose a scalar field.³ The cosmological constant is thought to be linked to the universe's vacuum energy—the minimum energy of a system. For this model, the vacuum energy, or vacua, is represented by the minimum of the potential. Only stable minima are of interest. Oscillations from this position, called perturbations, are postulated to be the theoretical explanation for the expansion seen in the universe. In this report, the mathematical representation of this potential field will be studied using quadratic and cubic potential fields. Also, perturbation theory will be discussed in numerical examples.

The Probability Distribution

A probability distribution was used to ascertain the likelihood of a particular potential's minima achieving a specified certain value in the field. For simplicity, it was assumed that the field propagates only in one dimension and is invariant to alterations in time.

In any given potential of a single field, the coefficients are independent of each other. In order to achieve the most general solution to the probability distribution, the coefficients are randomized through a probability distribution. In this case, each coefficient is assumed have a uniform distribution in the interval $[0, 1]$ which is our region of interest. This region was selected for its simplicity as any distribution can be used to determine peaking behavior. It is believed that the peaking behavior is robust to alterations in the distribution of the random coefficients and the interval selected. As long as consistency is maintained, any reasonable range with a given distribution can be used to determine a specific field's probability to peak at zero.

The probability function then becomes:

$$P(V_{\min}) = \int_{a_{x_1}}^{b_{x_1}} \int_{a_{x_2}}^{b_{x_2}} \dots [f(x_1)f(x_2) \dots \delta(V_{\min} - (x_1 + x_2 + \dots))] dx_1 dx_2 \dots$$

Discussion of correlation

We will evaluate the correlation of the analytical solution to the numerical histogram via observation. Often approximations must be made to the analytical result in order to gain a useful equation for the probability distribution. These approximations will be compared with the numerical result for consistency, however, statistical tests will not be performed on the functions to determine the strength of the correlation.

Methodology

Numerical analysis

As the probability distribution for functions become more complicated, numerical analysis becomes essential for approximating the probability distribution—it can also be helpful in guessing the analytical result. One million iterations were performed in creating each graph. Using a pseudo-random number generator, Mathematica was used to generate numbers between 0 and 1 at random. After a random number was generated for each of the coefficients, they were tested and regenerated until they adhered to the stability criteria for the minima. The minima was then determined by imputing the values into the equation for the minimum and the result was cataloged in a table equal in size to the number of iterations. Finally, these results were plotted using Mathematica's Histogram function within a specified interval, which included zero, and plotted using the "PDF" mode with a specified resolution.

Analytic analysis

For the Analytical result, the equation describing the probability distribution as a function of the potential value was generated via direct calculation of the above probability distribution function. The importance of the analytic result resides in its ability to represent these probability distributions by functions which are well understood.

Results and Discussion

Basic functions and their distributions

Before continuing to discuss the probability distribution, several functions were studied numerically to determine the peaking behavior of various polynomial

minima. Important results with the numerical examples are represented below.

Polynomial functions with the following form showed peaking behavior:

$$n = a^{n+k}, \text{ where } k \geq 1 \quad (1)$$

Additionally, functions of interest for later analysis are depicted by the following graphs.

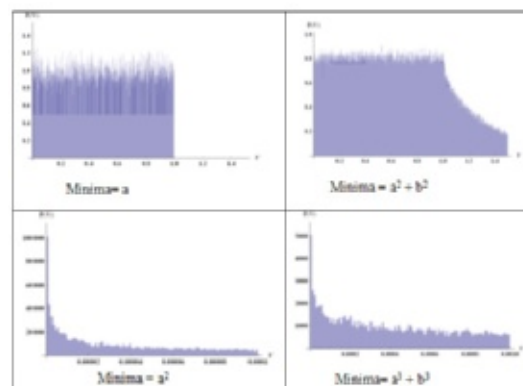


Table 1. Comparative peaking and non-peaking plots of simple minima to demonstrate numerical peaking analysis.

Single fields

Quadratic case:

To introduce the methods of solution and analysis, let us discuss the simplest case: a quadratic potential in one field.

$$\text{The potential is: } V = ax + bx^2 \quad (2)$$

The minimum occurs at

$$x = -\frac{a}{2b} \quad \text{where the constraint} = b > 0$$

Here is an overlay of the numerical and the analytic depictions of the quadratic case:

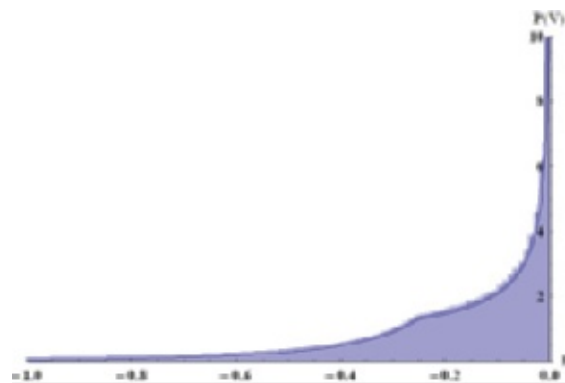


Figure 1. Numerical and Analytical probability distribution of a quadratic single field potential $V = ax + bx^2$ where a and b are random coefficients with uniform distribution from $[0,1]$

Features of interest are the turning point at $V = -1/4$. This cannot be explained via the numerical result however the analytic result gives important insight into understanding this condition. The probability function is:

$$P(V) = \int_0^1 \int_0^1 \delta\left(v + \frac{a^2}{4b}\right) db da \quad \text{which results in} \quad \begin{cases} \frac{1}{12\sqrt{3}} & V \leq -\frac{1}{4} \\ \frac{2}{3\sqrt{3}} & -\frac{1}{4} < V < 0 \end{cases} \quad (3)$$

Where v represents all possible values of the potential and the delta function selects for values of a and b which satisfy the minimum condition.

This demonstrates that the turning point can be represented as a shift between two functions and shows the power of acquiring an analytical solution to any given probability distribution.

Cubic Case:

For the cubic case, the potential is:

$$V = ax + bx^2 + cx^3 \quad (4)$$

In the cubic case, there are two minima with the included stability condition:

$$V_{\min} = \frac{(b + \sqrt{b^2 - 3ac})(b^2 - 6ac + b\sqrt{b^2 - 3ac})}{27c^2}; \quad \text{where } x = \frac{-b - \sqrt{b^2 - 3ac}}{3c}; \quad \text{constraint} = \sqrt{b^2 - 3ac} < 0 \quad (5)$$

$$V_{\min} = \frac{(-b + \sqrt{b^2 - 3ac})(-b^2 + 6ac + b\sqrt{b^2 - 3ac})}{27c^2}; \quad \text{where } x = \frac{-b + \sqrt{b^2 - 3ac}}{3c}; \quad \text{constraint} = \sqrt{b^2 - 3ac} > 0 \quad (6)$$

In the first case, the solution the constraint condition is excluded from this system since a , b , and c were set to be real. Therefore the second condition was chosen for analyzing the peaking behavior.

The resulting plot is show here:

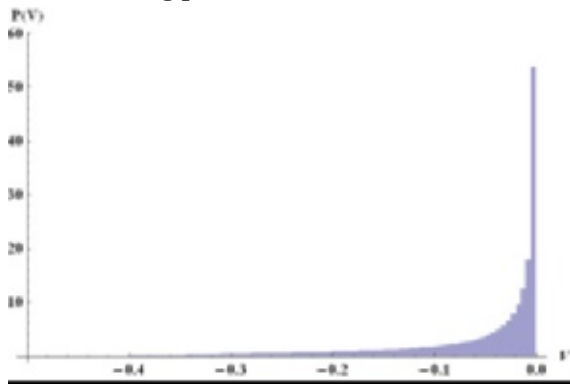


Figure 2. Numerical probability distribution of a cubic single field potential $V = ax + bx^2 + cx^3$ where a , b and c are random coefficients with uniform distribution from $[0, 1]$

There is no turning point described in the numerical plot, however peaking still approaches zero from the negative side.

Cubic Perturbations:

Below are the results of the numerical analysis of the Cubic Perturbations. Values for the perturbative coefficient (the coefficient in front of the x^3 term) were selected from 1 to .01, where the coefficient is uniform distribution in the interval $[0, 1]$.

Each constant value is listed under each graph, all other parameters were not changed.

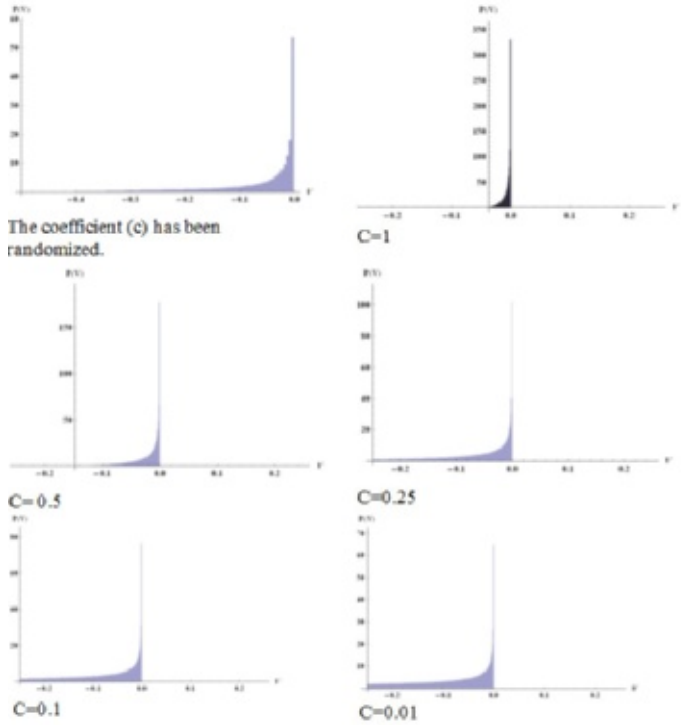


Table 2. Numerical probability distribution of a cubic single field potential $V = ax + bx^2 + cx^3$ where a and b are random coefficients with uniform distribution from $[0, 1]$. C is being treated perturbatively to observe the shifting probability distributions away from zero.

From the above results, we see that as the perturbations decrease, the peaking behavior is not affected, however, the width of the peak increases. These demonstrates that quadratic single field potentials show a lower probability of peaking at zero as the perturbations increase. From the expression of the quadratic potential, it is possible that as the coefficient for the cubic term decreases, there is a term which is added to the analytical expression of the quadratic potential causing the probability of peaking at zero to decrease. the quadratic potential causing the probability of peaking at zero to decrease.

Bi Fields

In this analysis, the fields are assumed to be fully decoupled. It is trivial to prove that by matrix diagonalization any coupled field can be represented

as two decoupled potentials. The same analysis that was performed on the single field distributions can be repeated with the bi fields since the resulting coefficients from decoupling will be approximately uniform in the interval $[0,1]$. The resulting expressions, or combinations of the coefficients, are represented by Greek letters which are approximated to be uniform in the interval $[0, 1]$.

Quadratic Case:

In this case:

$$V = ax + bx^2 + cy + dy^2 + exy \quad (7)$$

In the decoupled form:

$$V = \alpha x + \beta x^2 + \gamma y + \delta y^2 \quad (8)$$

where the Greek letter corresponds to the decoupled form of the corresponding, coupled Arabic letter. It is assumed that with full decoupling, the respective Greek letters are still approximately uniform from $[0, 1]$.

The minimum conduction occurs when

$$\text{Minima} = -\frac{\alpha^2}{4\beta} - \frac{\gamma^2}{4\delta} \quad (9)$$

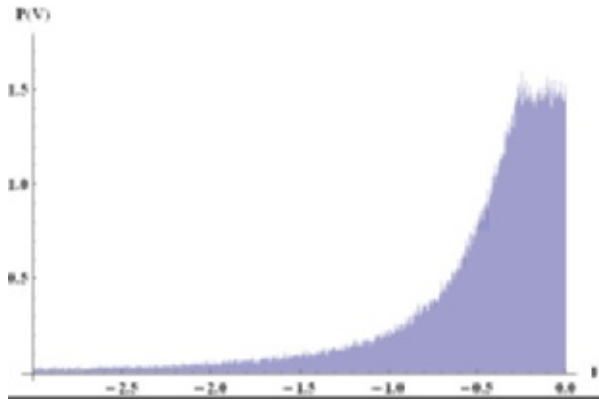


Figure 3. Numerical probability distribution of a quadratic bi-field potential $V = ax + bx^2 + cy + dy^2$ where a, b, c and d are random coefficients with uniform distribution from $[0, 1]$

With the addition of a second field, the peaking behavior of the potentials is obliterated. Obviously there is a conflict between the potentials generated by each of the two fields resulting in the peak leveling-off as zero is approached. It is interesting to note that the probability distribution exists only for negative values of the potential.

Cubic Case:

The equation for the potential is:

$$V = kx + lx^2 + mx^3 + ty + oy^2 + py^3 + qxy + sxy^2 + rx^2y \quad (10)$$

Following decoupling this becomes:

$$V = Ax + Bx^2 + Hx^3 + Ly + My^2 + Fy^3 \quad (11)$$

where $A, B, H, L, M,$ and F are Uniform in the interval $[0, 1]$. Only the positive roots were selected from the four

equations for the minima since the requirement that the random variables be real excludes all minima with negative roots. Therefore the resulting expressions are as follows:

$$x \rightarrow \frac{-B + \sqrt{B^2 - 3AH}}{3H}; y \rightarrow \frac{-M + \sqrt{M^2 - 3LF}}{3F} \quad (12)$$

The constraint conditions are:

$$\sqrt{B^2 - 3AH} > 0 \text{ and } \sqrt{M^2 - 3LF} > 0 \quad (13)$$

The expression for the minimum is therefore:

$$\frac{1}{27F^2H^2} (2B^3F^2 - 9ABF^2H - 2B^2F^2\sqrt{B^2 - 3AH} + H(6AF^2\sqrt{B^2 - 3AH} + H(2M^2(M - \sqrt{-3FL + M^2}) + FL(-9M + 6\sqrt{-3FL + M^2})))) \quad (14)$$

Although this case looks quite similar to the single field potential for the Cubic field, peaking behavior was not observed.

Next, the values of the perturbative constants were fixed and the resulting potentials are shown in two ways: First, the coefficients were reduced by the same amount; Second, one coefficient was fixed at 0.5 while the other was reduced. The resulting potentials are shown below were the constants are C and H . The V , defined by the positive roots of both, x and y was used to create this result.

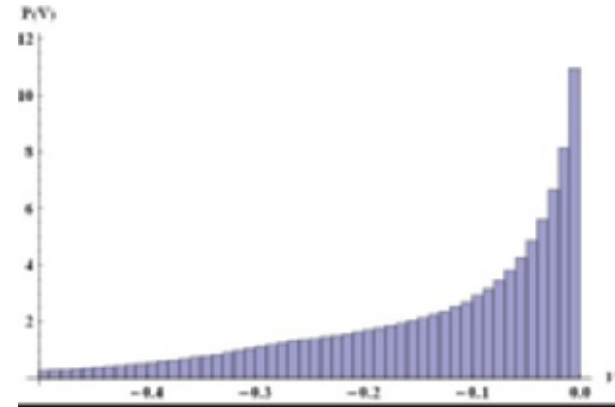


Figure 4. Numerical probability distribution of a cubic bi-field potential: $V = Ax + Bx^2 + Hx^3 + Ly + My^2 + Fy^3$ where $A, B, H, L, M,$ and F are random coefficients with uniform distribution from $[0, 1]$. V is described by the positive root of both fields.

For both cases, the peaking behavior was reduced as the probability spread more evenly over the interval shown and the turning point which appeared in the quadratic potential becomes more apparent as the C and H coefficients are reduced. It is interesting to note that this turning point in the cubic bi field was located at a more negative V value than the turning point in the quadratic single field potential (where $V = -1/4$).

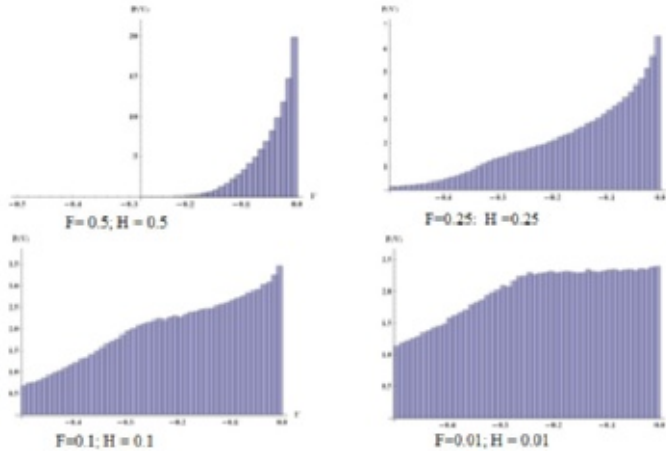


Table 3. Numerical probability distribution of a cubic bi-field potential $V=Ax+Bx^2+Hx^3+Ly+My^2+Fy^3$ where $A, B, L,$ and M are random coefficients with uniform distribution from $[0, 1]$. $H,$ and F are treated perturbatively in a uniform manner to observe the shifting probability distributions away from zero

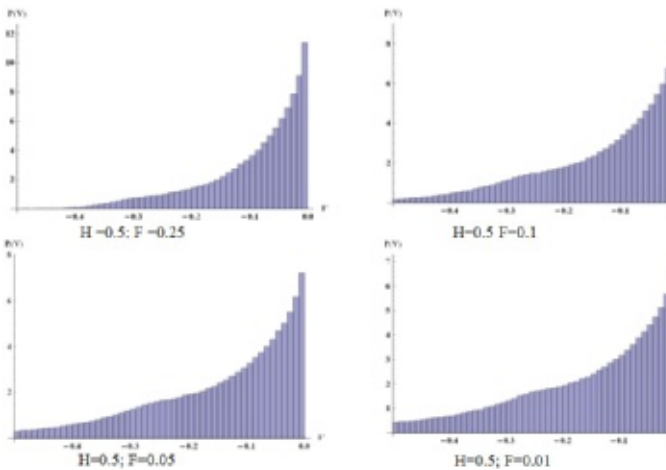


Table 4. Numerical probability distribution of a cubic bi-field potential $V= ax + bx^2 + cx^3 + dy + ey^2 + fy^3$ where $a, b, d,$ and e are random coefficients with uniform distribution from $[0, 1]$. H is held constant while F is treated perturbatively to observe the shifting probability distributions away from zero.

Conclusion and Future Work

Polynomial potentials are an interesting topic of study in creating mathematical representations for cosmological effects. Perturbations to the quadratic potential can simulate the oscillations which the universe takes around its stable minima or vacuum energy. These perturbations can affect gravity causing expansions and contractions in the size of the universe. In this study, these perturbations decreased the probability of the potential peaking at zero. Additionally, the cubic bi-field potential

shifted the turning point seen in the quadratic single field potential. Possibly, the shift in the turning point location could be analogous to the universe's vacuum energy selecting a different value. If so, then the shift in the turning point could represent the universe's change in size, which would explain the expansion seen today and would predict that infinite expansion is unlikely.

For future work, analytical solutions for the quadratic and cubic bi-field will be developed to deepen our understanding of the probability curves. Additionally, perturbations to the cubic potential will be studied via analysis of quartic potentials.

References

1. S. Weinberg, "Anthropic Bound on the Cosmological Constant," *Physics Review Letters*. 59 (1987) 2607.
2. Planck Collaboration, "Planck 2013 Results. XVI. Cosmological Parameters," *arXiv: 1303.5076*, *Astronomy & Astrophysics* (2013).
3. S. Weinberg, "A Priori Probability Distribution of the Cosmological Constant," *Physics Review*. D61 (2000) 103505, *arXiv:astro-ph/0002387* [astro-ph].

1 kb regions of MALAT1 and NEAT1 are sufficient for RNA nuclear retention

Laura Y. Lu¹, Jeremy E. Wilusz², Phillip A. Sharp²

¹Student Contributor, Class of 2014, Department of Biology, Massachusetts Institute of Technology (MIT), Cambridge, MA 02139, USA

²David H. Koch Institute for Integrative Cancer Research, MIT, Cambridge, MA 02139, USA.

³David H. Koch Institute for Integrative Cancer Research, and Department of Biology, MIT, Cambridge, MA 02139, USA.

Supplemental information is available online for this report.

MALAT1 (metastasis-associated lung adenocarcinoma transcript 1) and NEAT1 (nuclear enriched abundant transcript 1, also known as MEN ϵ / β) are long noncoding RNAs that, when misregulated, have been implicated in a variety of human diseases including metastatic cancer, aberrant synaptogenesis, and HIV. Little is known about the functions of these RNAs, but recent studies show that they localize to specific structures within the nucleus: MALAT1 to nuclear speckles and NEAT1 to nuclear paraspeckles. In the current study, we aimed to identify sequence elements within MALAT1 and NEAT1 that are sufficient to cause a reporter mRNA to be retained in the nucleus. By screening reporter plasmids containing various fragments of these noncoding RNAs, we identified ~1 kb regions within MALAT1 and NEAT1 that are sufficient for RNA nuclear retention in HeLa cells. We further found that the efficiency of nuclear retention rapidly decreases as the size of the inserted region is decreased. Surprisingly, certain MALAT1 fragments additionally appear to function as translational enhancer elements when inserted in the 5' UTR of the reporter plasmid. These results suggest a complex and intricate mechanism for specific nuclear retention of MALAT1 and NEAT1 and suggest additional, unexplored functions for these RNAs.

Introduction

RNA expression and localization play a dynamic role in regulating cell function. More specifically, certain RNAs appear to have many important functions in the nucleus, as they have been shown to regulate X-chromosome inactivation in mammals, alternative pre-mRNA splicing, and formation of diverse nuclear structures (reviewed by Heard and Disteche, 2006, Tripathi et al., 2010, Sunwoo et al., 2009). Several studies have demonstrated that misregulation and aberrant localization of such RNAs play a significant role in human disease. For example, myotonic dystrophy type 1 (DM1) is associated with

the accumulation of mutant mRNA transcripts in the neuronal nucleus, which leads to depletion of certain proteins in the cytoplasm, as well as the abnormal regulation of alternative splicing for a distinct set of neuronal pre-mRNAs (Jiang et al., 2004).

Similarly, several studies have implicated the misregulation of certain long noncoding RNAs (lncRNAs) with a breadth of human diseases. These RNAs are sometimes highly evolutionarily conserved but many of their functions remain mysterious as they lack apparent protein-coding function, yet are associated with diseases such as Huntington's Disease, HIV-1, and many human carcinomas (Johnson, 2011, Zhang et al., 2013, Lin et al.,

2006). A greater understanding of how these RNAs are regulated and localized may elucidate the broader role of RNA in gene expression and embryogenesis (Lecuyer et al., 2007, Prasanth et al., 2005). Furthermore, characterization of RNA localization has the potential for providing new therapeutic targets and strategies, such as correcting human mitochondrial diseases and preventing cancer metastasis (Wang et al., 2012, Ji et al., 2003, Ying et al., 2012).

In particular, MALAT1 (metastasis associated lung adenocarcinoma transcript 1) and NEAT1 (nuclear enriched abundant transcript 1, also known as MEN ϵ/β), two nuclear-retained ncRNAs, specifically localize to nuclear speckles and paraspeckles, respectively. Nuclear speckles contain a distinct set of pre-mRNA splicing regulators involved in exon recognition and alternative splicing (Lamond and Spector, 2003, Nakagawa et al., 2012). There, MALAT1 has been found to regulate splicing factors known as serine/arginine-rich proteins (SR proteins), thereby modulating alternative splicing and gene expression patterns. Although the molecular details are unclear, MALAT1 misregulation appears to play a critical role in promoting metastasis of non-small cell lung cancer and bladder cancer (Tripathi et al., 2010, Yang et al. 2011, Ji et al., 2003, Ying et al., 2012, Wilusz et al., 2008). Interestingly, NEAT1 is encoded in the human genome directly next to MALAT1, although the

RNA localizes to a completely different nuclear domain known as paraspeckles, where it functions as an essential structural component (Sunwoo et al., 2008, Zhang et al., 2013).

Although the downstream effects of MALAT1 and NEAT1 localization clearly affect splicing of certain mRNAs and thus downstream gene expression, the molecular mechanisms by which these long ncRNAs are retained in the nucleus are still unknown. As such, the goal of this research project is to determine the molecular mechanisms by which long noncoding RNAs are retained in the nucleus and how they localize to specific nuclear structures. In particular, we aim to understand how MALAT1 localizes to nuclear speckles and how NEAT1 localizes to nuclear paraspeckles. By transfecting HeLa cells with a reporter plasmid containing various fragments of MALAT1 or NEAT1, we worked to identify the minimal sequences that are necessary and sufficient for RNA nuclear retention and localization to specific nuclear structures. In the current study, we identified ~1 kb regions in MALAT1 and NEAT1 that are sufficient for nuclear retention of reporter mRNA and found that various fragments of these two noncoding RNAs result in a dynamic range of mRNA nuclear retention. Surprisingly, our results suggest that certain MALAT1 fragments may additionally function as translational enhancer elements.

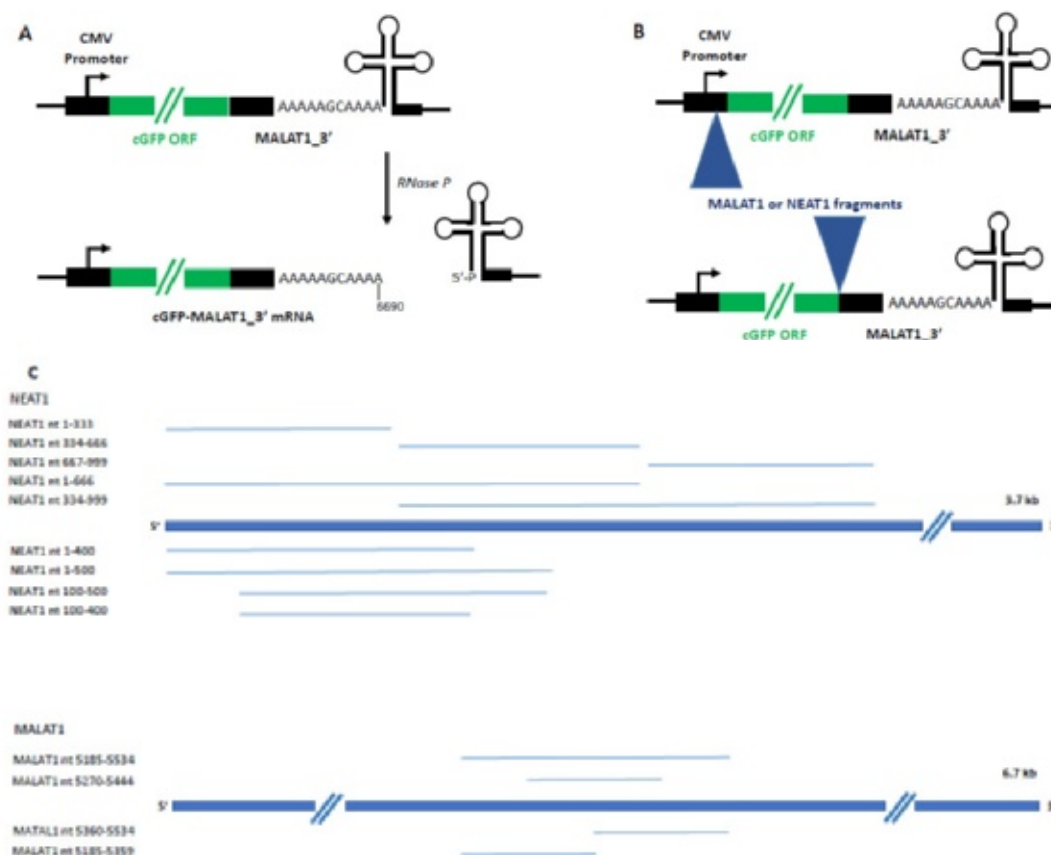


Figure 1. The CMV-cGFP-MALAT1_3' expression plasmid recapitulates the non-canonical 3' end processing of MALAT1 (Wilusz et al., 2008). MALAT1 is primarily processed via a cleavage mechanism mediated by the tRNA biogenesis machinery. The mature MALAT1 transcript is generated by RNaseP cleavage upstream of a tRNA-like structure (A). Plasmids were constructed by inserting fragments of MALAT1 or NEAT1 either upstream or downstream of the cGFP ORF to screen for nuclear retention elements (B). Various fragments of NEAT1 and MALAT1 were inserted into the expression plasmid to generate 17 nuclear retention constructs (C).

Results

To validate that our expression system is suitable for identifying nuclear retention elements, we first determined the nuclear/cytoplasmic ratio of the cGFP mRNA generated from a previously described mammalian expression plasmid (Wilusz et al. 2012, Figure 1a), in which a CMV promoter drives the expression of coral green fluorescent protein (cGFP). Downstream of the cGFP ORF, the MALAT1_3' region (MALAT1 nt 6581-6754) was inserted, allowing a non-canonical 3' end processing mechanism to occur that nonetheless results in production of a stable cGFP mRNA that can be efficiently translated in cells (Figure 1a). This vector was transfected into HeLa cells, and both protein and RNA were extracted 24 hours post-transfection. The RNA was further fractionated into nuclear and cytoplasmic fractions, which were subjected to Northern blot analysis to determine the RNA distribution between the nucleus and cytoplasm. Reporter cGFP protein expression was detected by Western blot. In the vector alone, there was reporter cGFP protein expression (Figure 2a) as well as efficient RNA export to the cytoplasm (Figure 2b). From these results, we determined that this expression system was suitable for identifying nuclear retention elements since we could detect a dynamic range of cGFP protein expression as well as nuclear-cytoplasmic mRNA distribution.

Using this system, we generated 17 expression constructs that had various regions of NEAT1 or MALAT1 inserted in the vector to identify the nuclear retention elements of these two noncoding RNAs. NEAT1 (Supplemental Table 1) and MALAT1 (Supplemental Table 2) fragments (Figure 1c) were inserted either upstream or downstream of the cGFP ORF (Figure 1b), and their sequence, sense orientation, and insertion location were verified by sequencing. As previously described, we detected cGFP protein expression and nuclear-cytoplasmic mRNA distribution to determine

whether certain NEAT1 and MALAT1 regions were sufficient for nuclear retention of reporter mRNA.

Insertion of NEAT1 fragments upstream of the cGFP ORF often results in RNA instability

In a previous study, we identified a 1 kb region of NEAT1 (NEAT1 nt 1-1000) that is sufficient for nuclear retention when inserted in the 5' UTR of our expression plasmid (Figure 2b). Other studies posit that specific localization sequences may be as small as 20 nt in length (Wang et al., 2010); hence, we attempted to systematically narrow down the 1 kb region of NEAT1 to identify the minimal sequences necessary for nuclear retention. First, we generated three constructs with 333 nt insertions of NEAT1 in the 5' UTR of the expression plasmid and transfected them into HeLa cells. The insertion of the NEAT1 elements resulted in a loss of cGFP protein expression (Figure 2a). To determine if the loss of protein expression was a result of nuclear retention (increased levels of RNA in the nuclear fraction) of the reporter transcript, we performed Northern blots to compare the levels of cGFP mRNA in the cytoplasmic and nuclear fractions (Figure 2b). As expected, the 1 kb region resulted in efficient nuclear retention as there was almost no cGFP mRNA detected in the cytoplasm (Figure 2b); however, compared to the vector alone, there was little total RNA detected, suggesting that the reporter transcript was unstable. Similarly, minimal reporter RNA was detected for the third 333 nt construct (NEAT1 nt 667-999), implying that the fragment insertion likely caused RNA instability and degradation. In the first third 333 nt construct (NEAT1 nt 1-333), we observed some nuclear retention as more RNA (~1.5 fold) was detected in the nuclear fraction than in the cytoplasmic fraction. On the other hand, the middle third (NEAT1 nt 334-666) showed efficient RNA export to the cytoplasm, similar to vector (cGFP-MALAT1_3') nuclear and cytoplasmic RNA levels. From these observations, we found that

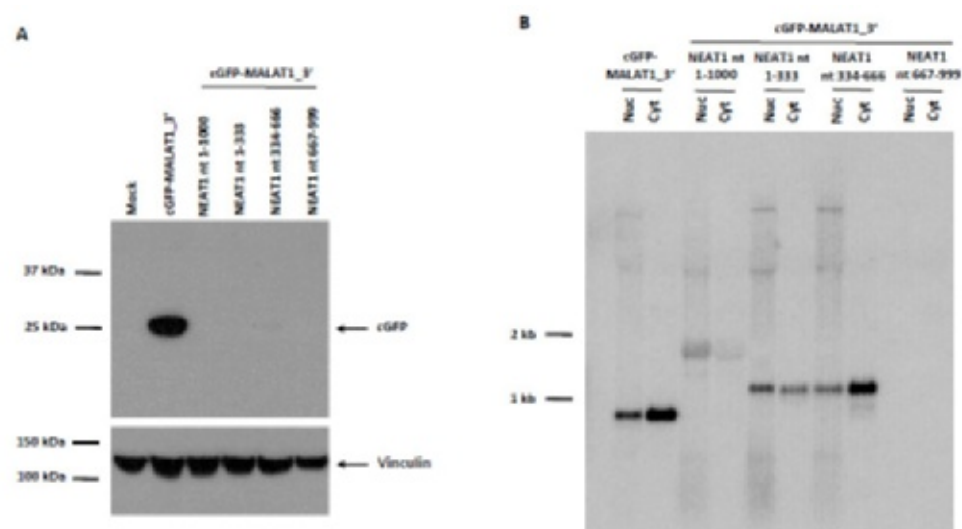


Figure 2. When the various fragments of NEAT1 were inserted upstream of the cGFP ORF, a loss of cGFP protein expression was observed. Fragments 333 nt in length were inserted upstream of the cGFP ORF in the expression construct to generate the NEAT1-cGFP-MALAT1_3' constructs. Western blot was used to detect cGFP expression of transfected HeLa cells, and a vinculin antibody was used as a loading control (A). A probe complementary to the cGFP ORF was used to detect nuclear (Nuc) and cytoplasmic (Cyt) RNA in transfected HeLa cells by Northern blotting (B).

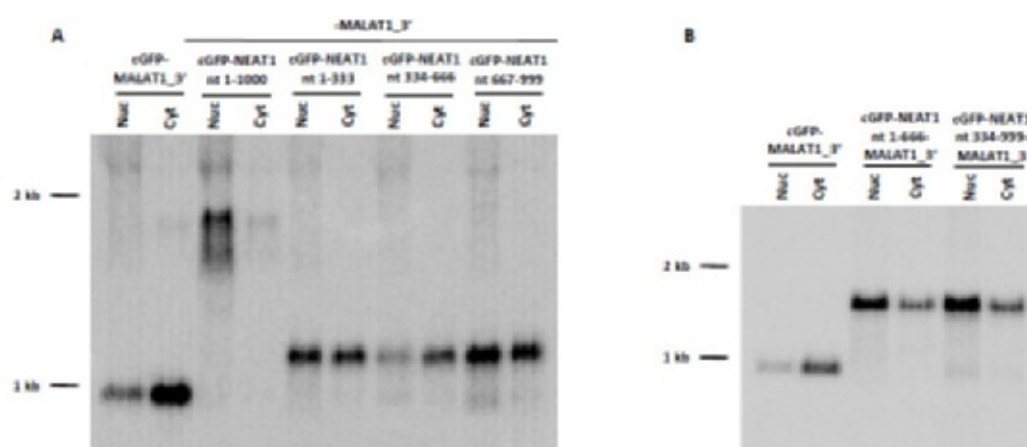


Figure 3. Nuclear retention was observed when 333 nt and 666 nt NEAT1 fragments were inserted downstream of the cGFP ORF. Constructs in which 333 nt (A) and 666 nt (B) fragments derived from the NEAT1 nt 1-1000 region were generated and transfected into HeLa cells. Northern blots were used to detect nuclear (Nuc) and cytoplasmic (Cyt) RNA using a probe complementary to cGFP.

333 nt NEAT1 insertions in the 5' UTR results in RNA instability.

Insertion of a 1 kb region of NEAT1 downstream of the cGFP ORF is sufficient for efficient nuclear retention

As these 5' UTR insertion constructs seemed to compromise RNA stability, we generated expression plasmids with the same fragments, but inserted them in the 3' UTR. Moreover, as it seemed that there was decreased nuclear retention efficiency with decreased NEAT1 fragment size, we also generated two 666 nt fragments derived from the same 1 kb region of NEAT1. With these constructs we found that RNA stability was improved compared to the constructs with the 5' UTR 333 nt inserts, and the 1 kb region allowed for almost full nuclear retention of the reporter transcript (Figure

3a). Similarly, the NEAT1 nt 1-333 and NEAT1 nt 667-999 constructs showed some degree of nuclear retention (~1.5-fold more RNA in the nuclear fraction than in the cytoplasmic fraction), though the RNA was at a lower expression level than the 1 kb region (Figure 3a). Again, the middle NEAT1 nt 334-666 region showed efficient RNA export to the cytoplasm comparable to that of the vector alone (Figure 3a). Consistent with the higher nuclear retention efficiency of the 1 kb 5' UTR construct than for the shorter inserts, the longer 666 nt fragments caused more efficient nuclear retention (Figure 3b) of the reporter RNA than the 333 nt fragments, as more RNA was detected in the nuclear fraction than in the cytoplasmic fraction in the 666 nt constructs.

We then performed Western blots to assess the effects of these varying RNA nuclear retention levels on protein expression. Similar to findings with the 1 kb NEAT1 insertion in the 5' UTR, no cGFP protein was detected for the 1 kb NEAT1 region construct (Figure 4) since the RNA was efficiently nuclear retained. Varying levels of protein expression were observed for the rest of the NEAT1 constructs consistent with their associated nuclear retention efficiencies. That is, for constructs that retained more RNA in the nucleus compared to the cytoplasm, less cGFP protein was detected. For example, low levels of protein expression were observed for the NEAT1 nt 1-333 and both 666 nt constructs. As these constructs efficiently retained more reporter RNA in the nucleus than in the cytoplasm (Figure 3a, Figure 3b), a reduction in protein expression (Figure 4) would be expected. Further, less protein was detected for the 666 nt constructs than for the NEAT1 nt 1-333 construct since the reporter RNA was more efficiently nuclear retained in the longer 666 nt constructs (Figure 4). As the NEAT1 nt 334-666 construct had efficient RNA export to the cytoplasm (Figure 3a), cGFP protein levels similar to the vector protein levels were observed (Figure 4). Together, these data suggest a direct correlation between nuclear retention efficiency and fragment length; as the size of

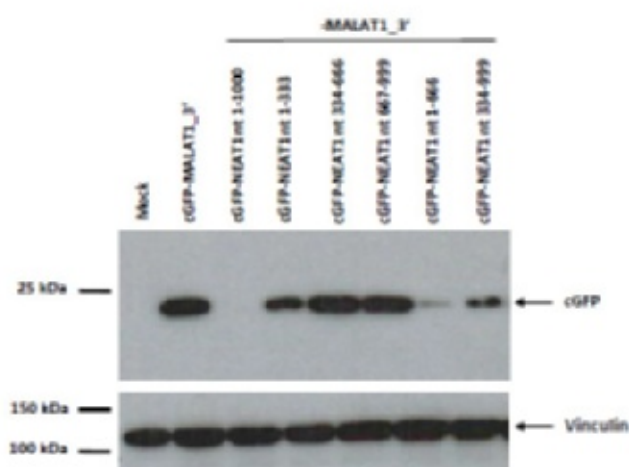


Figure 4. Reduced cGFP protein expression was observed with insertion of NEAT1 fragments downstream of the cGFP ORF. Constructs of 333 nt and 666 nt fragments derived from the 1 kb NEAT1 nuclear retention region were generated and transfected into HeLa cells. Western blots were used to detect cGFP expression of transfected HeLa cells, and a vinculin antibody was used as a loading control.

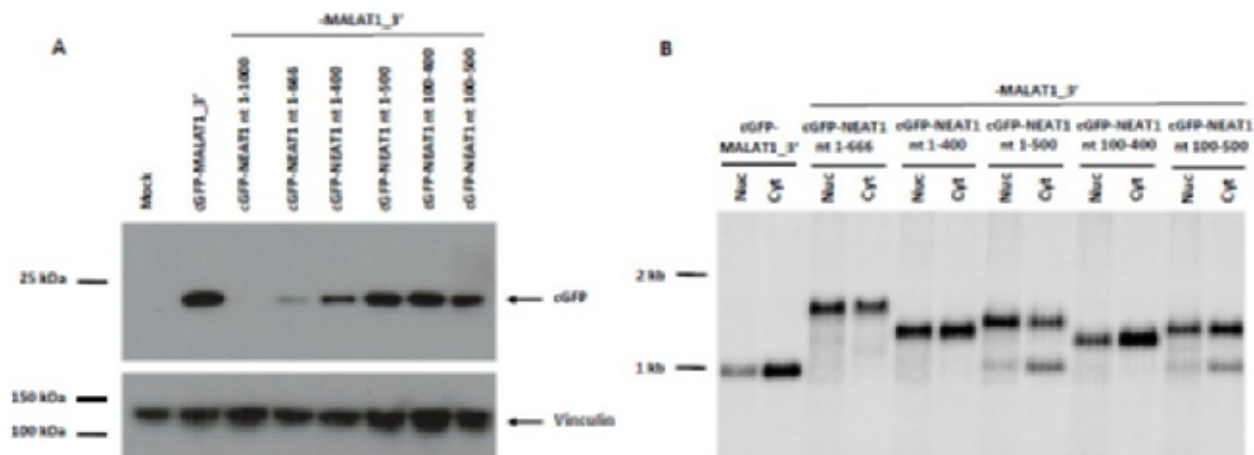


Figure 5. Insertion of certain NEAT1 fragments downstream of the cGFP ORF resulted in a range of reduced cGFP protein expression. Constructs containing 300, 400, 500, or 666 nt fragments derived from the 1 kb NEAT1 nuclear retention region were generated and transfected into HeLa cells. Western blot was used to detect cGFP expression of transfected HeLa cells, and a vinculin antibody was used as a loading control (A). Northern blot was used to detect nuclear (Nuc) and cytoplasmic (Cyt) RNA using a probe complementary to cGFP (B). Expected RNA sizes ranged from 1 kb to ~1.7 kb depending on the size of the NEAT1 fragment inserted.

the insertion decreases, the nuclear retention efficiency is reduced. However, we cannot exclude changes in RNA structure as the primary determinant of nuclear retention.

To further narrow down the NEAT1 nuclear retention elements, we generated expression plasmids with 300, 400, and 500 nt NEAT1 fragments. Since longer NEAT1 regions seemed to cause more efficient nuclear retention, we created the 400 and 500 nt constructs as intermediate lengths between the previously described 333 and 666 nt inserts. We generated the 300 nt NEAT1 insert because inclusion of the 5' end of the 1 kb NEAT1 region seemed to be important for nuclear retention of the reporter transcript. After transfecting HeLa cells, we again observed a dynamic range of protein expression for the different constructs (Figure 5a). All of these new NEAT1 constructs had less protein expression than the vector but more protein expression than the longer NEAT1 nt 1-666 construct (Figure 5a). Furthermore, the two 400 nt constructs (NEAT1 nt 1-400 and NEAT1 nt 100-500) had more cGFP protein expression than the NEAT1 nt 1-666 but less protein expression than the 300 nt and 500 nt constructs (Figure 5a). Here too, we observed that the length of inserted NEAT1 fragments generally correlated inversely with protein expression.

We then assessed nuclear and cytoplasmic RNA distributions to determine whether the protein expression levels aligned with nuclear retention of the reporter RNA. Unlike the 333 nt and 666 nt constructs, the nuclear retention efficiencies of the 400 and 500 nt constructs did not correspond with their associated cGFP protein levels (Figure 5b). Both the NEAT1 nt 1-400 and the NEAT1 nt 1-500 constructs were nuclear retained while

the NEAT1 nt 100-400 and NEAT1 nt 100-500 construct RNAs were efficiently exported to the cytoplasm (Figure 5b). Moreover, additional, shorter RNAs were detected for the NEAT1 nt 1-500 and NEAT1 nt 100-500 constructs (Figure 5b), suggesting that splicing events may occur with these NEAT1 constructs, thereby possibly complicating the interpretation of our results.

Overall, we confirmed that a 1 kb region of NEAT1 is sufficient for nuclear retention of a reporter RNA and found that nuclear retention efficiency decreases

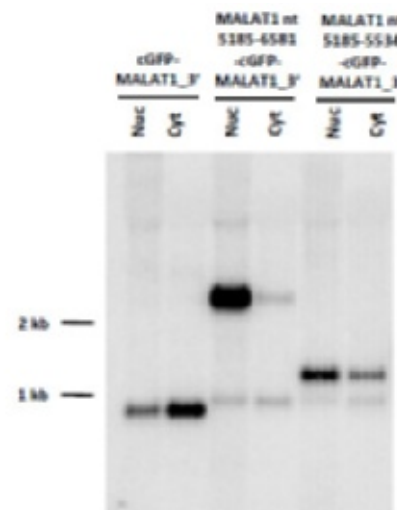


Figure 6. Nuclear retention was observed upon insertion of MALAT1 fragments upstream of the cGFP ORF. MALAT1 regions 1.4 kb and 350 nt in length were inserted upstream of the cGFP ORF to generate expression plasmid constructs that were transfected into HeLa cells. Northern blot was used to detect nuclear (Nuc) and cytoplasmic (Cyt) RNA with a probe complementary to cGFP.

with shorter fragment insertions in the 3' UTR of the expression plasmid. We also observed that increased nuclear retention resulted in decreased protein expression as less RNA was exported to the cytoplasm for translation.

Insertion of a 1.4 kb region of MALAT1 upstream of the cGFP ORF is sufficient for efficient nuclear retention

Using the same process we had applied for NEAT1, we aimed to systematically narrow down the previously identified 1.4 kb nuclear retention element of MALAT1 (MALAT1 nt 5185-6581). A 350 nt MALAT1 (MALAT1 nt 5185-5534) region was inserted in the 5' UTR of the expression plasmid, and the amounts of reporter transcript in the nuclear and cytoplasmic fractions were determined by Northern blot analysis (Figure 6). Nuclear retention was observed in this construct as more RNA (~3 fold) was detected in the nuclear fraction than in the cytoplasmic fraction (Figure 6). The 1.4 kb MALAT1 construct had efficient nuclear retention (Figure 6), with almost total nuclear retention of the reporter RNA.

To further narrow down the 350 nt MALAT1 region, we generated three 175 nt MALAT1 constructs derived from this 350 nt region: the first 175 nt (MALAT1 nt 5185-5359), the last 175 nt (MALAT1 nt 5360-5534), and the middle 175 nt (MALAT1 nt 5270-5444) of this 350 nt region were inserted in the 5' UTR of the expression plasmid. We found that the first 175 nt MALAT1 fragment had some level of nuclear retention (~1:1 nuclear to cytoplasmic RNA ratio) (Figure 7a), though this retention was less efficient than for the 350 nt construct, which exhibited ~ 3-fold difference

in nuclear versus cytoplasmic RNA levels (Figure 7a). On the other hand, the other two 175 nt constructs (MALAT1 nt 5360-5534 and MALAT1 nt 5270-5444) did not show reporter transcript nuclear retention or reporter transcript stability (Figure 7a). Similar to NEAT1, these results indicate that reducing the length of MALAT1 insertions reduces nuclear retention efficiency and reporter transcript stability.

Various MALAT1 fragments may function as translational enhancer elements

We then detected cGFP protein expression to determine the relationship between reporter RNA localization and protein expression. Unlike in the NEAT1 system, we observed the same amount of protein expression (Figure 7b) in the 1.4 kb MALAT1 construct as the vector alone despite the high nuclear retention efficiency of the 1.4 kb construct (Figure 7a). Even more surprisingly, all the MALAT1 constructs had increased cGFP protein levels compared to the vector (Figure 7b), suggesting that the 5' UTR MALAT1 inserts may act as translational enhancer elements. Unlike the NEAT1 constructs, insertion of the MALAT1 fragments upstream of the cGFP ORF led to higher protein expression regardless of the nuclear retention or stability of the reporter RNA.

In summary, using the same approach we employed for NEAT1, we identified a ~1.4 kb region of MALAT1 that is sufficient for nuclear retention of a cGFP reporter transcript. Similar to what we observed for NEAT1, we found that, in general, reducing the size of MALAT1 insertions led to decreased nuclear retention efficiency. Interestingly, we found that certain insertions of MALAT1

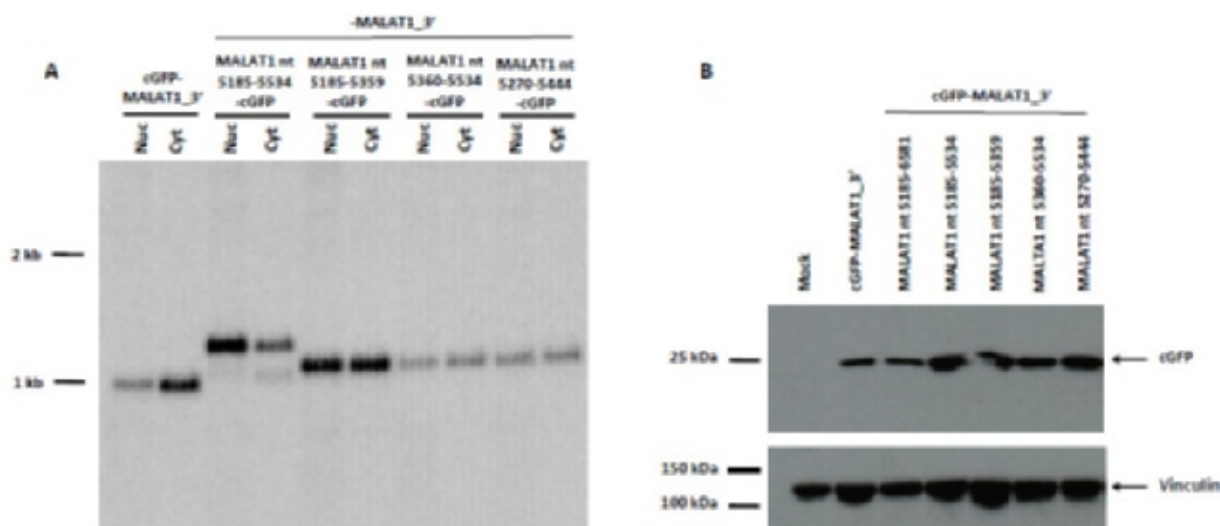


Figure 7. Insertion of 175 nt fragments of MALAT1 upstream of the cGFP ORF was not sufficient for nuclear retention and resulted in increased cGFP protein expression. Three 175 nt fragments derived from the MALAT1 nt 5185-5534 region were inserted in the 5' UTR of the expression plasmid to generate expression constructs that were transfected into HeLa cells. A probe complementary to cGFP was used in Northern blot to detect nuclear (Nuc) and cytoplasmic (Cyt) RNA of transfected HeLa cells (A). Western blot was used to detect cGFP expression of transfected HeLa cells, and a vinculin antibody was used as a loading control (B).

resulted in increased protein expression, suggesting these regions may function as translational enhancer elements.

Discussion

Many RNAs exhibit specific localization patterns within the cell, suggesting that their function goes beyond merely serving as intermediates between DNA and protein. In particular, MALAT1 and NEAT1 (also known as MEN ϵ/β), two noncoding RNAs, have been shown to localize to specific nuclear structures and, as a result, modulate alternative splicing patterns and gene expression (Lamond and Spector, 2003, Tripathi et al., 2010, Yang et al. 2011). Although this specific subcellular localization affects splicing of certain mRNAs, the fundamental question of how these RNA transcripts localize to the nucleus remains unanswered. What sequences, structures, and proteins are necessary for the RNA nuclear localization mechanism? How does this localization affect downstream processes, such as subsequent protein expression?

In the present study, we identified regions of NEAT1 and MALAT1 that are sufficient for nuclear retention. Specifically, we identified a 1 kb region of NEAT1 (NEAT1 nt 1-1000) that efficiently retains a reporter RNA in the nucleus when inserted either upstream or downstream of the expression plasmid cGFP ORF. Similarly, we identified a 1.4 kb region of MALAT1 (MALAT1 nt 5185-6581) that is sufficient for nuclear retention of cGFP reporter RNA when inserted in the 5' UTR of the expression plasmid. In trying to identify minimal nuclear retention sequences, we found that nuclear retention efficiency rapidly decreased with the shorter NEAT1 and MALAT1 fragment insertions and that, for NEAT1, increased nuclear retention efficiency led to decreased cGFP protein expression. Interestingly, insertion of certain MALAT1 fragments in the 5' UTR caused increased protein expression, suggesting that these MALAT1 sequences may function as translational enhancer elements.

Taken together, these results indicate that the nuclear retention mechanisms for both NEAT1 and MALAT1 are complex and significantly different from other well-understood nuclear retention mechanisms. For example, CTN-RNA, which is produced from the mouse cationic amino acid transporter 2 (mCAT2) gene locus, contains a stretch of inverted repeats in its 3' UTR, which causes CTN-RNA to form an intramolecular hairpin structure (Prasanth et al., 2005). This hairpin structure targets the RNA for A-to-I editing and subsequent nuclear retention (Prasanth et al., 2005). Interestingly, the CTN-RNA hairpin is post-transcriptionally cleaved off upon cellular stress, and this modification allows the RNA to be exported to the cytoplasm for translation. Via a possibly similar

mechanism, aberrant myotonic dystrophy protein kinase (DMPK) mRNA contains a CUG trinucleotide expansion in its 3' UTR that causes the formation of a hairpin structure (Davis et al., 1997). This stable structure causes the mutant DMPK transcript to aggregate in the nucleus and lose its ability to be transported to the cytoplasm for translation (Mastroiannaopoulos et al., 2012). The lack of inverted repeats, A-to-I editing, and trinucleotide expansions in either NEAT1 or MALAT1 indicate that the nuclear retention mechanisms of both these RNAs are distinct from that of CTN-RNA as well as mutant DMPK mRNA (Prasanth et al., 2005, Davis et al., 1997, Mastroiannaopoulos et al., 2010).

Furthermore, the dynamic range of nuclear retention efficiency of various insertions of NEAT1 and MALAT1 does not match the binary nuclear retention phenotypes observed for CTN-RNA. For CTN-RNA, the absence of the intramolecular hairpin causes a loss of nuclear retention and promotes efficient RNA export to the nucleus for translation of the mCAT2 protein (Prasanth et al., 2005). In contrast to this conserved nuclear retention sequence, several NEAT1 fragments of varying length, from 333 nt to 1 kb, can confer a range of nuclear retention when inserted in the 3' UTR of the expression plasmid. This dynamic range suggests that there may be several distinct regions or dispersed smaller sequences within the 1 kb nuclear retention region of NEAT1 that are essential for efficient nuclear retention. Alternatively, proteins involved in the nuclear localization mechanism may introduce specific structural constraints that require the full 1 kb region for efficient nuclear retention.

It is perhaps not surprising that a relatively long region (~1 kb) is required for efficient nuclear retention of NEAT1 and MALAT1. A longer nuclear localization sequence may allow for increased specificity of the nuclear retention mechanisms used by these two long noncoding RNAs. If the nuclear localization sequences were shorter, like the 20 nt stem loop described by Wang and colleagues (Wang et al., 2010), there would be a higher probability that more RNA transcripts would have the 20 nt sequence, and thus an increased number of transcripts would be retained in the nucleus. Instead, the long length suggests a more specific mechanism that allows for the unique functions associated with the nuclear retention of MALAT1 and NEAT1.

Surprisingly, our findings suggest that certain MALAT1 fragments may function as translational enhancer elements. This, in turn, might suggest that MALAT1 may encode for peptides, contrary to the expectations of a nuclear-retained RNA but consistent with our recent work showing that the triple helix present at the 3' end of MALAT1 is able to function in translation (Wilusz et al. 2012). We found that the insertion of certain MALAT1 fragments in the 5' UTR of our expression

plasmid caused increased protein expression regardless of reporter RNA localization. Similarly, we observed that even the 1.4 kb region of MALAT1 that results in almost total nuclear retention shows protein expression comparable to the vector alone, which has efficient RNA export to the cytoplasm. This promotes the idea that these fragments may function as translational enhancer elements, though it is curious that an RNA, which apparently lacks protein-coding ability, would enhance translation and thus protein expression in our reporter plasmid. Previous studies have shown that there are small ORFs that do not start with the canonical AUG start codon that encode for short, unprocessed peptides that have key biological functions (Galindo et al., 2007). Together with our findings, this observation suggests that MALAT1 may not only enhance translation but also encode for small peptides, although MALAT1 has previously been identified as a noncoding RNA (Ji et al., 2003).

Although we have identified sequences that promote nuclear retention, it remains to be determined if these sequences are necessary for specific localization within the nucleus to nuclear speckles and paraspeckles for MALAT1 and NEAT1, respectively. Our current data only confirms that certain reporter RNAs are nuclear retained, but future RNA FISH and microscopy could determine the specific localization of the reporter RNAs within the nucleus. As we have yet to visualize the localization of these nuclear retained RNAs, some of the RNA instability and reduced nuclear retention efficiency observed in our study could be a result of mislocalization within the nucleus. That is, localization to either the paraspeckles or speckles may tether the RNAs to the nuclear structure, and loss of this localization could allow these RNAs to escape the nucleus. This observation would suggest that the nuclear retention and paraspeckle/ speckle localization signals may be distinct. In other words, there may be separate mechanisms that first drive nuclear retention and then specific localization within the nucleus.

Even though the nuclear retention mechanisms for MALAT1 and NEAT1 remain unclear, our current work provides a strong foundation for possibly exploiting these nuclear retention sequences as therapeutic targets and tools. Bioinformatic analysis may reveal if similar sequences are found elsewhere in the human transcriptome. Such sequences might be useful as therapeutic targets for preventing cancer metastasis of non-small cell lung cancer, which is associated with the upregulation of MALAT1 (Ji et al., 2003). By targeting the nuclear retention signal sequence specific for MALAT1, we may be able to degrade these excess MALAT1 transcripts and thus reduce the chance of cancer metastasis. By a different approach, we might

fuse the NEAT1 nuclear retention sequences to mRNAs that are upregulated in certain diseases, such as metastatic cancer, to prevent the excess mRNAs from being exported to the cytoplasm for translation. By sequestering these mRNAs in the nucleus, cancer growth and progression could be stifled as the protein product of the upregulated mRNAs would not be produced. Other similar subcellular localization signals could be exploited as Wang et al. (2012) succeeded in reversing functional defects in mitochondrial RNA translation as well as respiration by fusing a 20 nt mitochondria-directing stem loop to a nuclear-encoded RNA to complement the mitochondrial defect. Moreover, once we gain a better understanding of the mechanism and proteins involved in nuclear retention of certain RNAs, we might find ways to inhibit these proteins from retaining certain RNA in the nucleus. For example, we could potentially introduce a mutant RNase that cleaves the nuclear retention signal sequence and thus allows these RNAs to be exported out to the cytoplasm for translation. Our identification of MALAT1 and NEAT1 nuclear retention elements provide a powerful foundation for potential therapeutic strategies against a variety of human diseases.

In this study, we identified nuclear retention elements in the long noncoding RNAs NEAT1 and MALAT1 that are sufficient for nuclear retention by transfecting HeLa cells with expression plasmids that included various NEAT1 and MALAT1 fragments. Further analysis of this type may broaden our understanding of MALAT1 and NEAT1 regulation and nuclear localization, as well as the greater phenomenon of RNA localization mechanisms and their associated downstream effects, such as resulting protein expression. This understanding provides insights and potential for new therapeutic strategies such as altering RNA localization for a wide breadth of human diseases, including Huntington's Disease, HIV-1, and many human carcinomas (Johnson, 2011, Zhang et al., 2013, Lin et al., 2006).

Materials & Methods

Expression plasmid construction

To generate the CMV-NEAT1-cGFP-MALAT1_{3'} and CMV-cGFP-NEAT1-MALAT1_{3'} expression constructs, a previously described plasmid (Wilusz et al., 2012) was modified to clone in fragments of NEAT1 both upstream and downstream of the cGFP ORF. NEAT1 regions (Supplemental Table 1) were inserted into the EcoRV and SalI cloning sites in the sense direction to generate the CMV-NEAT1-cGFP-MALAT1_{3'} and the CMV-cGFP-NEAT1-MALAT1_{3'} expression plasmids, respectively. Similarly, MALAT1 regions (Supplemental Table 2) were inserted into the EcoRV cloning site in the sense direction to generate the CMV-MALAT1-

cGFP-MALAT1_3' constructs. These constructs were transformed into One Shot TOP10 E. coli (Life Technologies), and plasmid DNA was purified using the PureYield Plasmid Miniprep System (Promega) following manufacturers' protocols. The miniprep silica-membrane column allowed for selective DNA binding in high salt concentrations. To ensure correct orientation of NEAT1 and MALAT1 insertions, miniprep samples were sequenced by the Koch Institute Sequencing Facility, and correct expression plasmids were purified by the EndoFree Plasmid Purification Maxi Kit (Qiagen) following the manufacturer's modified alkaline lysis procedure and anion-exchange resin column protocol.

Transfections and RNA analysis

Twenty-four hours prior to transfection, HeLa cells were grown at 37°C with 5% CO₂ in Dulbecco's modified Eagle's medium (DMEM) containing high glucose (Life Technologies), supplemented with penicillin-streptomycin and 10% fetal bovine serum (FBS). The expression plasmids were transfected using Lipofectamine 2000 (Life Technologies) as per manufacturer's protocol. Cellular fractionation was performed to isolate nuclear and cytoplasmic RNA from the transfected cells. Cells were trypsinized, centrifuged, and lysed with 1 mL of Lysis Buffer B (10 mM Tris-HCl pH 8-8.4, 140 mM NaCl, 1.5 mM MgCl₂, 0.5% NP40, 0.35% SUPERase-In RNase Inhibitor by Ambion, 1mM DTT) 24 hours post-transfection. The samples were spun for 3 minutes at 4°C, and 650 µL of the supernatant, representing the cytoplasmic fraction, was transferred to a new tube and placed on ice. The remaining pellets were resuspended in Lysis Buffer B, and 100 µL of detergent stock (3.3% Sodium deoxycholate, 6.6% Tween 40) was added drop-by-drop under slow vortexing. The samples were incubated on ice for 5 minutes and then spun for 3 minutes at 4°C. The supernatant was discarded, and the pellet was resuspended in Lysis Buffer B and centrifuged for 3 minutes at 4°C. Again, the supernatant was discarded and the pellet remaining represented the nuclear fraction. The cytoplasmic and nuclear RNA were isolated using Trizol (Life Technologies) following manufacturer's protocol. Northern blots probed for cGFP were performed by Jeremy Wilusz as previously described (Wilusz et al., 2008).

Protein Analysis

Twenty-four hours after transfection, HeLa cells were washed with PBS and placed on ice. After addition of 100 µL RIPA Buffer (10 mM Tris pH 7.4, 150 mM NaCl, 1% Triton X-100, 0.1% SDS, 0.5% Na-deoxycholate, 1 mM EDTA, 2% EDTA-free protease inhibitor cocktail by Roche), cells were scraped off of the plates and transferred to tubes. The samples were incubated on ice

for 10 minutes and centrifuged for 10 minutes at 4°C. After spinning, the supernatant was transferred to new tubes containing 50 µL of NuPAGE LDS Sample Buffer (Life Technologies) and 20 µL of NuPAGE Denaturing Agent (Life Technologies). The protein samples were incubated at 70°C for 10 minutes to denature the protein. Western blots were performed using the NuPAGE Bis-Tris electrophoresis system (Life Technologies), using 4-12% Bis-Tris polyacrylamide gels to separate protein. Primary antibodies used were cGFP antibody (GenScript) at 1:10,000 dilution and Vinculin antibody (Sigma-Aldrich) at 1:1,000 dilution.

Acknowledgments

The authors wish to dedicate this paper to the memory of Officer Sean Collier, for his caring service to the MIT community and for his sacrifice. I would also like to thank Professor Phillip Sharp, Dr. Jeremy Wilusz, and other members of the Sharp Laboratory for their mentorship, helpful guidance, and thoughtful discussion throughout this project. Further, I am grateful for the instruction and advice of Professor Susan Lindquist and Dr. Leslie Roldan.

References

1. Davis, B.M., McCurrach, M.E., Taneja, K.L., Singer, R.H., and Housman, D.E. (1997). Expansion of a CUG trinucleotide repeat in the 3' untranslated region of myotonic dystrophy protein kinase transcripts results in nuclear retention of transcripts. *Proc. Natl. Acad. Sci. U. S. A.* 94, 7388-7393.
2. Galindo, M.I., Pueyo, J.I., Fouix, S., Bishop, S.A., and Couso, J.P. (2007). Peptides encoded by short ORFs control development and define a new eukaryotic gene family. *PLoS Biol.* 5, e106.
3. Heard, E., and Distech, C.M. (2006). Dosage compensation in mammals: fine-tuning the expression of the X chromosome. *Genes Dev.* 20, 1848-1867.
4. Ji, P., Diederichs, S., Wang, W., Boing, S., Metzger, R., Schneider, P.M., Tidow, N., Brandt, B., Buerger, H., Bulk, E., et al. (2003). MALAT-1, a novel noncoding RNA, and thymosin beta4 predict metastasis and survival in early-stage non-small cell lung cancer. *Oncogene* 22, 8031-8041.
5. Jiang, H., Mankodi, A., Swanson, M.S., Moxley, R.T., and Thornton, C.A. (2004). Myotonic dystrophy type 1 is associated with nuclear foci of mutant RNA, sequestration of muscleblind proteins and deregulated alternative splicing in neurons. *Hum. Mol. Genet.* 13, 3079-3088.

6. Johnson, R. (2012). Long non-coding RNAs in Huntington's disease neurodegeneration. *Neurobiol. Dis.* 46, 245-254.
7. Lamond, A.I., and Spector, D.L. (2003). Nuclear speckles: a model for nuclear organelles. *Nat. Rev. Mol. Cell Biol.* 4, 605-612.
8. Lecuyer, E., Yoshida, H., Parthasarathy, N., Alm, C., Babak, T., Cerovina, T., Hughes, T.R., Tomancak, P., and Krause, H.M. (2007). Global analysis of mRNA localization reveals a prominent role in organizing cellular architecture and function. *Cell* 131,174-187.
9. Lin, R., Maeda, S., Liu, C., Karin, M., and Edgington, T.S. (2007). A large noncoding RNA is a marker for murine hepatocellular carcinomas and a spectrum of human carcinomas. *Oncogene* 26, 851-858.
10. Mastroyiannopoulos, N.P., Shammas, C., and Phylactou, L.A. (2010). Tackling the pathogenesis of RNA nuclear retention in myotonic dystrophy. *Biol. Cell.* 102, 515-523.
11. Nakagawa, S., and Hirose, T. (2012). Paraspeckle nuclear bodies--useful uselessness? *Cell Mol. Life Sci.* 69, 3027-3036.
12. Prasanth, K.V., Prasanth, S.G., Xuan, Z., Hearn, S., Freier, S.M., Bennett, C.F., Zhang, M.Q., and Spector, D.L. (2005). Regulating gene expression through RNA nuclear retention. *Cell* 123, 249-263.
13. Sunwoo, H., Dinger, M.E., Wilusz, J.E., Amaral, P.P., Mattick, J.S., and Spector, D.L. (2009). MEN epsilon/beta nuclear-retained non-coding RNAs are up-regulated upon muscle differentiation and are essential components of paraspeckles. *Genome Res.*19, 347-359.
14. Tripathi, V., Ellis, J.D., Shen, Z., Song, D.Y., Pan, Q., Watt, A.T., Freier, S.M., Bennett, C.F., Sharma, A., Bubulya, P.A., et al. (2010). The nuclear-retained noncoding RNA MALAT1 regulates alternative splicing by modulating SR splicing factor phosphorylation. *Mol. Cell* 39, 925-938.
15. Wang, G., Chen, H.W., Oktay, Y., Zhang, J., Allen, E.L., Smith, G.M., Fan, K.C., Hong, J.S., French, S.W., McCaffery, J.M., et al. (2010). PNPASE regulates RNA import into mitochondria. *Cell* 142, 456-467.
16. Wang, G., Shimada, E., Zhang, J., Hong, J.S., Smith, G.M., Teitell, M.A., and Koehler, C.M. (2012). Correcting human mitochondrial mutations with targeted RNA import. *Proc. Natl. Acad. Sci. U. S. A.* 109, 4840-4845.
17. Wilusz, J.E., Freier, S.M., and Spector, D.L. (2008). 3' end processing of a long nuclear-retained noncoding RNA yields a tRNA-like cytoplasmic RNA. *Cell* 135, 919-932.
18. Yang, L., Lin, C., Liu, W., Zhang, J., Ohgi, K.A., Grinstein, J.D., Dorrestein, P.C., and Rosenfeld, M.G. (2011). ncRNA- and Pc2 methylation-dependent gene relocation between nuclear structures mediates gene activation programs. *Cell* 147, 773-788.
19. Ying, L., Chen, Q., Wang, Y., Zhou, Z., Huang, Y., and Qiu, F. (2012). Upregulated MALAT-1 contributes to bladder cancer cell migration by inducing epithelial-to-mesenchymal transition. *Mol. Biosyst* 8, 2289-2294.
20. Zhang, Q., Chen, C.Y., Yedavalli, V.S., and Jeang, K.T. (2013). NEAT1 long noncoding RNA and paraspeckle bodies modulate HIV-1 posttranscriptional expression. *Mbio* 4, e00596-12.

Salinity and Density in Deep Boreholes

William DeMaio¹, Ethan Bates²

¹Student Contributor, Class of 2016, Department of Nuclear Science and Engineering, Massachusetts Institute of Technology (MIT), Cambridge, MA 02139, USA

²Department of Nuclear Science and Engineering, Massachusetts Institute of Technology (MIT), Cambridge, MA 02139, USA

In deep borehole nuclear waste disposal, waste canisters are exposed to high temperatures, pressures, and salinities. While a canister's ability to withstand these conditions and delay water contact with the spent nuclear fuel (SNF) is important, canisters eventually compromise (relative to the decay timescale) and the soluble contents dissolve into the surrounding water. Subsequently, the decay heat could drive vertical convective flows and transport of radionuclides to the surface and humans. Existing density gradients (due to salinity, for example) can offset the thermal buoyancy driving force for convective flow, rendering the fluid system stable and stagnant. Data on the chemical composition of these fluids (from boreholes drilled across the globe) is available to about 2000m; however, it has not been previously used to assess convection in deep boreholes. Based on an extensive literature search, various curve fits for salinity vs. depth are developed in this paper. In addition, a number of density vs. salinity relationships are reviewed, accounting for variations in salt chemistry. Based on the best fit to salinity data obtained from the Canadian Shield, density vs. depth can be approximated by $\rho = (7.08 \times 10^{-4} \pm 1.5 \times 10^{-4}) \times (0.1234 \times \text{Depth(m)})^2 - 59.419 \times \text{Depth(m)} + 5844.6 + \rho_{\text{ref}}$ to ~2000m. In combination, the resulting depth dependent relationship allows for accurate assessment of the importance of salinity in the deep borehole concept while accounting for the inherent uncertainty of such data. This range of curves has use in estimating the effects of salinity on the prevention of thermal convection and therefore the transport of dangerous radionuclides upwards from spent nuclear fuel repositories.

Introduction

With the de-funding of the Yucca Mountain Nuclear Waste Repository, the United States remains in need of a nuclear waste disposal solution. The lack of safe, feasible options for spent nuclear fuel (SNF) disposal could potentially set back the nuclear energy industry (Slovic et al., 1991). Deep boreholes have been identified as a potential answer to at least part of the nuclear waste problem, but more assurances are required before boreholes can be used for waste disposal. For instance, buoyant flows are a potential mechanism by which long-lasting radionuclides could reach the surface after escaping from a compromised canister (Kukkonen, 1995). In order to understand and quantify the risks associated with such escape mechanisms, the chemical composition of the groundwaters surrounding the canisters must be examined, especially because of the strong effects

dissolved ions can have on the physical properties of water, including density and viscosity (Millero et al., 1980; Zhang et al., 1997). Both of these variables can greatly affect the flow of water upwards, and need to be understood for accurate and representative models to be created. Therefore, the need arises for an examination of the data obtained from existing borehole studies.

Overview of prior work

In order to predict various effects that groundwaters will have on deep geological SNF repositories, the properties and chemistries of such groundwaters must also be predicted. Unfortunately, relationships between salinity and depth are not well modeled, especially within the context of deep boreholes. Additionally, many papers on waste disposal either make very simplifying

assumptions, or ignore the effects of the salinity gradient completely due to an inability to model it simply.

For example, one paper from 1989 specifically on fluid density in deep boreholes states “When major geochemical variations take place with depth, total dissolved solids may be the single most important factor in determining the density of the formation fluid; this is especially relevant when considering the wide range in total dissolved solids associated with salt deposits.... However, the variation of total dissolved solids content with depth is not a smooth function that can be predicted in a general case” (Oberlander, 1989). Salinity at the same depth can indeed vary by several orders of magnitude across the globe. However, the ability to generally predict, say, salinity with depth in North American granite has been written off prematurely. Additionally, the increasing availability of data from drilled boreholes at greater depths allows for more accurate relationships to be determined.

Other borehole-related studies make similar claims or use unexplained salinity curves that are not based on real-world data (Arnold and Hadgu, 2013; Hartley and AB, 2006). Clearly, analysis of the chemistry and origin of brines specific to borehole sites will be critical to the assurance of safety. Nevertheless, an approximate formulation of salinity and density with depth is a tool necessary for the modeling of deep borehole SNF disposal and its sensitivity to salinity gradients.

This paper attempts to reduce the need for simplifying assumptions about chemical composition and its variance with depth by analysis of deep groundwater data from around the world. Additionally, various density relationships will be incorporated to find an acceptable density with depth relationship suitable for computational codes.

Salinity variation with depth

Salinity has a number of potentially positive and negative effects in the deep borehole concept. It is an important contributor to corrosion rates, and a potential inhibitor of the swelling behavior of bentonite, a material being considered for use in repositories (Haug et al., 1988). Most importantly, the amount and type of these dissolved solids can determine subsurface flows via alteration of the density and viscosity of the water (Zhang et al., 1997). The groundwater chemistry could have other potentially important effects such as altering the precipitation of silica and healing of cracks, which have been identified as an important escape mechanism (Chaudhuri et al., 2008).

Research began by looking into the potential effects of natural salt precipitation as deep groundwater rises

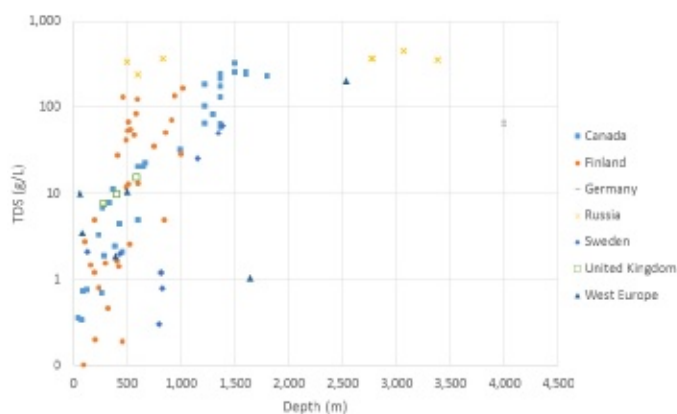


Figure 1. Semi-log plot of the salinities of water samples taken from borehole studies around the world. All data from (Frape et al., 2003) except for Canadian samples from 0-1000m [11]

through the geothermal gradient. There have been several attempts to understand and quantify this phenomenon, but it did not appear that anyone had looked into the potential benefits of salt precipitation as a negative feedback effect to the flow of heated water and brine, especially in the context of waste disposal (Chaudhuri et al., 2008). Early investigations focused on silica (SiO_2), which has a very low saturation limit in water, so its potential as an additive was intriguing. It was soon discovered that the solubility of silica is not well understood at high temperatures and pressures (Fournier and Rowe, 1977) (Weres et al., 1979). Chiefly, silica's deposition rate depended greatly on the other chemical features of the brine. Thus, among many other reasons, it was decided that granitic deep groundwater compositions needed to be typified before looking into the effects of specific substances at saturation.

Fortunately, chemical data from borehole samples is ever-increasing. As granite disposal facilities are widely seen as one of the most promising options for deep borehole SNF disposal, we focused on finding the typical composition of granitic groundwaters as well as their common inconsistencies. Data to be analyzed was sourced from two main groups: worldwide and the Canadian Shield. Helpful compilations of data points from individual experimental boreholes were provided by Frape, Gascoyne, and others (Frape et al., 2003; Gascoyne, 2004). The overall TDS (mass of total dissolved solids dissolved per liter of solution) of the data may be seen in Figure 1.

As the plot shows, great diversity exists among all of the data points. However, the regional variations appear to follow some relationship with depth, which we attempt to find. In particular, the Canadian Shield was focused upon because of both its geographical closeness to many potential United States deep borehole repositories and

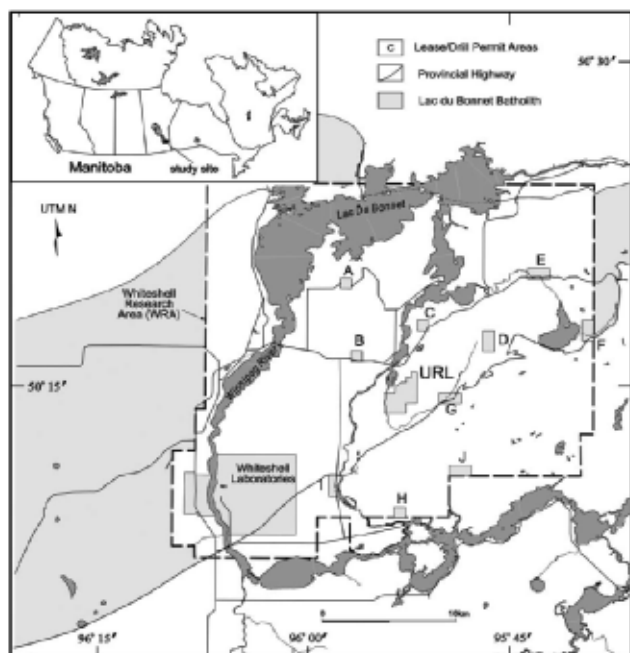


Figure 2. Location of the Gascoyne study (Gascoyne, 2004)

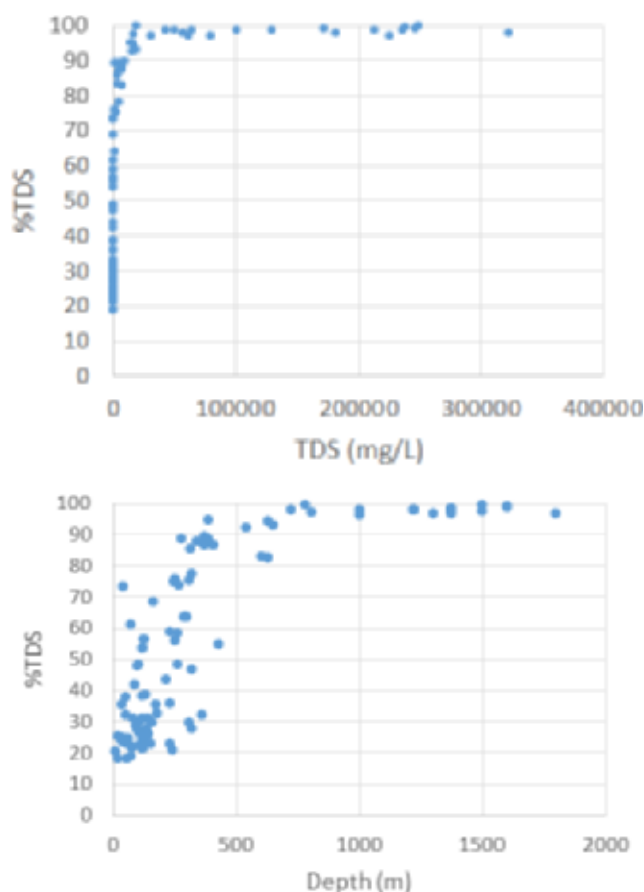


Figure 3. Percent of TDS made up by Na, Ca, and Cl ions vs. TDS and depth, respectively

the quality of the data. Notably, Gascoyne's tables include temperature and density measurements, which were not readily available for many boreholes in other countries.

Figure 3 shows the increasing proportion of TDS that is made up by NaCl and CaCl_2 . This finding is supported by Gascoyne, who concludes that the increased salinity is due either to interactions with the rock matrix and/or slow groundwater mixing (Gascoyne, 2004).

Next, an attempt was made to find a line of best fit through the Canadian data. The choice of a curve presumably has a great impact on predicted water density and therefore models of radionuclide transport, so multiple fits will be examined and discussed. These are shown in Figure 4.

As can be seen, the choice of curve fit will drastically affect the predicted values at deeper depths. This is partly due to the scarcity of data from boreholes much deeper than 1500 m, and also because of the variable nature of granitic brines. It is also critical to note that, based on relative concentrations of Na and Ca ions, the maximum TDS (as seen in deep groundwaters and discussed below) for water is in the range of 300-400 g/L. Therefore some of these lines of fit would reach maximums at around 1500 m, but with others this occurs at much deeper depths. It is clear that assumptions on salinity curves will drastically affect derived predictions, such as density.

Equations 1-4 are the curves of various types fitted to the TDS data (Table 1). If relevant, an estimated saturation point is given, and the R-squared values are shown for all equations.

It is important to note that, based on the temperatures expected in boreholes of this depth, the solubility limit of NaCl will be reached before that of CaCl_2 . This can be seen in Figure 5, where it is shown that the solubility of CaCl_2 due to temperature increases much faster than the concentration of CaCl_2 . Therefore, the brine will be unable to accept more NaCl before CaCl_2 is

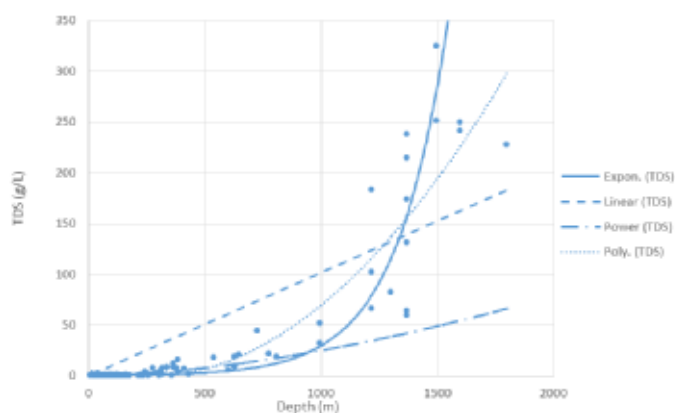


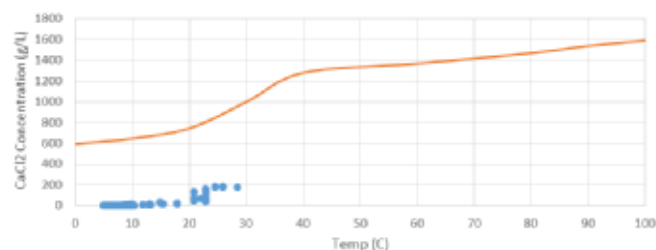
Figure 4. Various lines of fit to TDS and depth of data points from the Canadian Shield (Frape et al., 2003; Gascoyne, 2004)

Table 1. Projections of TDS with depth

Equation	Brine Depth (TDS = 350 g/L)	Saturation Depth (TDS = 1500g/L)	R^2	(Eqn.)
$TDS \left(\frac{mg}{L}\right) = 319.04e^{0.0045 \times Depth(m)}$	1500m	1900m	$R^2 = 0.861$	(1)
$TDS \left(\frac{mg}{L}\right) = 0.1234 \times Depth(m)^2 - 59.419 \times Depth(m) + 5844.6$	2000m	3700m	$R^2 = 0.8535$	(2)
$TDS \left(\frac{mg}{L}\right) = 0.2505 \times Depth(m)^{1.666}$	5000m		$R^2 = 0.7078$	(3)
$TDS \left(\frac{mg}{L}\right) = 101.69 \times Depth(m)$	3500m		$R^2 = 0.6812$	(4)

According to the data, the brine can be considered to have a ratio of 1:3 NaCl to CaCl₂ deeper than 1000m (Frape et al., 2003). Extrapolating this to the maximum solubility of NaCl at the likely temperatures seen at 4000m (60°C according to a linear extrapolation of the geothermal gradient found in Gascoyne's compilation of borehole studies), the limiting mass of total dissolved solids comes out to ~1500g/L. At these levels, CaCl₂ would still be below saturation (American Chemical Society (2006). However, this appears to be a limit that is never approached in the real world.

Typically, three main regions of salinity are observed in groundwater studies. The first is the shallow region, where groundwater regularly interacts with surface water and has a low TDS (<30g/L). The second region is more saline, and is usually where the greatest increase in salinity is observed. This is the region with which we are mainly concerned due to the presence of a strong gradient. Finally, at large depths, salinity tends to reach a maximum of ~350g/L (Frape et al., 1984, 2003; Gascoyne, 2004; Park et al., 2009). This value is consistent with the highest values of salinity seen in borehole studies to date,

**Figure 5.** Solubility of CaCl₂ with temperature, along with Canadian data to 1800m (American Chemical Society (2006), 2006; Frape et al., 2003; Gascoyne, 2004)

suggesting that higher TDS values are unlikely to occur. The depth at which each model in Table 1 reaches this likely maximum is given in the “brine depth” column.

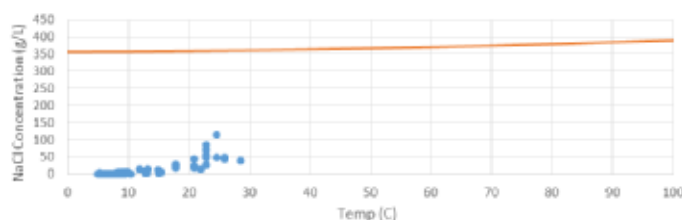
As is reflected in Figure 4 and the R² values, the exponential and polynomial relationships best account for the variability in the data. However, the extreme diversity of the predicted values and small amount of data make it unwise to draw conclusions about

any empirical relationship between salinity and depth. Nevertheless, the “spread” of these values can be used to determine the sensitivity of fluid flow models to the various salinity gradients.

Density variation with salinity

The increase of density with salinity is an important and beneficial phenomena with regards to inhibiting fluid convection in the deep borehole concept. In order to determine this effect, most previous works develop simplifying assumptions on the salt compositions and find a relationship between TDS and density, as is widely done with seawater (Kukkonen, 1995; Millero et al., 1980). Several of these formulations will be evaluated, along with their impact on the spread of predicted values. Note that no temperature or pressure effects are included here.

For the density curves, several previously determined relationships were used. Gascoyne's study of Canadian Shield groundwaters resulted in the best fit line seen

**Figure 6.** Solubility of NaCl with temperature, along with Canadian data to 1800m (American Chemical Society (2006), 2006; Frape et al., 2003; Gascoyne, 2004)

in (5). Because this curve was determined through experimental data, it fits the specific site very well, but there is the possibility that variances in the relative concentrations of dissolved solids could significantly affect density.

$$\rho = 7.95 \times 10^{-4} \times \text{TDS} \left(\frac{\text{mg}}{\text{L}} \right) + \rho_{\text{ref}} \quad (5)$$

This concern leads to the necessity of comparing several density relationships. Another method of relating these values was proposed by Millero for use with seawater (~35 g/L) and is widely accepted by that community.

$$(\rho - \rho_0) = AS + BS^{3/2} + CS^2 \quad (6)$$

With A, B, and C being functions of temperature (C) and salinity. These are given by:

$$\begin{aligned} A &= 8.24493 \times 10^{-1} - 4.0099 \times 10^{-3} T + 7.6438 \times 10^{-5} T^2 - 8.2467 \times 10^{-7} T^3 + 5.3875 \times 10^{-9} T^4 \\ B &= -5.72466 \times 10^{-3} + 1.0327 \times 10^{-4} T - 1.6546 \times 10^{-6} T^2 \\ C &= 4.8314 \times 10^{-4} \end{aligned}$$

(Millero et al., 1980). A simplification with A, B, and C constant for temperatures close to 20 °C is displayed in Equation (7).

$$\rho = 0.767535 \times \text{TDS} \left(\frac{\text{g}}{\text{L}} \right) - 4.3411 \times 10^{-3} \times \text{TDS} \left(\frac{\text{g}}{\text{L}} \right)^{3/2} + 4.8314 \times 10^{-4} \times \text{TDS} \left(\frac{\text{g}}{\text{L}} \right)^2 + \rho_{\text{ref}} \quad (7)$$

Equation (8) contains Kukkonen's approximation of density with dissolved solids, based on the assumption that all salts besides NaCl may be neglected (Kukkonen, 1995).

$$\rho = \rho_{\text{ref}} (1 + 5.6 \times 10^{-7} \times \text{TDS} \left(\frac{\text{mg}}{\text{L}} \right)) \quad (8)$$

It can also be shown that using mass fraction of individual dissolved salts will lead to Equation (9), where a_i is an empirically determined constant for each salt (0.73g/ml for NaCl and 0.85g/ml for CaCl₂), and m_i is the mass fraction of the salt species (Fritz and Frape, 1982; Laliberte and Cooper, 2004; Zhang et al., 1997). Of some importance is the fact that this relationship does not depend directly on TDS, but instead on the concentrations of individual salts. This may lead to a less accurate prediction if concentrations are assumed to be of some constant proportion.

$$\rho = \sum_i a_i m_i + \rho_{\text{ref}} \quad (9)$$

By assuming that relative NaCl and CaCl₂ concentrations agree with the ratios seen in borehole studies below 500m, a more general equation can be found. The mean concentrations used were: Na is 13.6% of the total TDS, with Ca at 23.3% and Cl at 63.1%. One must also assume that other ions are negligible, which is a fair assumption made by several authors above, especially when it is seen that these three ions make up 96% of the total dissolved mass on average (Kukkonen,

1995). One further assumption made to reduce the model includes a correct distribution of Cl ions to form salts. This is necessary because the density equation uses dissolved salts, but chemistry studies can only determine ion concentrations. This will be the source of some error, as when applied to known data it can be seen that Equation (10) occasionally presumes more dissolved mass present than is claimed by the TDS. However, this error appears to be small based on correlations to other density formulations and the low frequency with which it appears with known data.

$$\rho = \frac{0.242272 \times \text{TDS} \left(\frac{\text{mg}}{\text{L}} \right)}{3.31879 \times 10^{-4} \times \text{TDS} \left(\frac{\text{mg}}{\text{L}} \right) + \rho_{\text{ref}}} + \frac{0.526474 \times \text{TDS} \left(\frac{\text{mg}}{\text{L}} \right)}{6.19381 \times 10^{-4} \times \text{TDS} \left(\frac{\text{mg}}{\text{L}} \right) + \rho_{\text{ref}}} + \rho_{\text{ref}} \quad (10)$$

As seen in Figure 5. Comparison of various density with TDS formulations, these various formulations have a significant spread. It is becoming apparent that many assumptions will need to be made in order to develop a relationship between depth and density. As said in Section 4, depending upon relative concentrations of NaCl and CaCl₂, solutions usually do not have a TDS much higher than 350g/L.

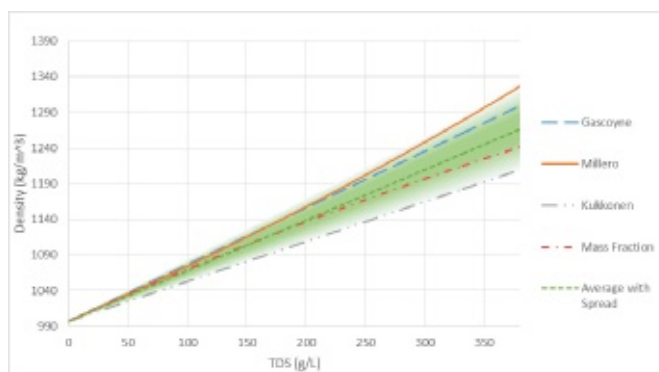


Figure 5. Comparison of various density with TDS formulations

In order to simplify the use of these models, we have used the linear approximation of these curves to formulate an average density with salinity relationship and a spread that accounts for most variability in chemical composition. This is given in Equation (11) and shown as “Average with Spread” in Figure 5.

$$\rho = (7.08 \times 10^{-4} \pm 1.5 \times 10^{-4}) \times \text{TDS} \left(\frac{\text{mg}}{\text{L}} \right) + \rho_{\text{ref}} \quad (11)$$

Discussion

Combining the relationships between total dissolved solids with depth, and density with total dissolved solids, it is possible to calculate the density of water with depth and demonstrate the spread created by model uncertainty. The most inclusive method for doing so is to combine the lowest and highest curves for each relationship. In addition to a range of values, it is also

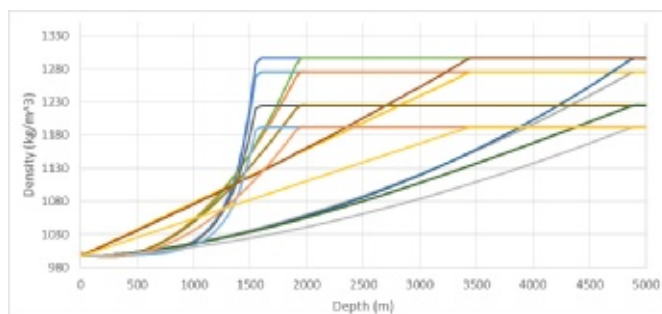


Figure 6. Projected density with depth curves

useful to have a “best guess,” an intermediate curve using the most well-founded relationships between the variables.

The main purpose of the following models is to typify the change in density due to TDS in the range of depth before the groundwater reaches its maximum salinity. Therefore, the salinity limit discussed in Section 4 of 350g/L has been imposed on each of the curves. The depth at which this limit is projected to be reached varies between models, and is likely an important consideration for deep borehole repositories. The total spread along with every discussed relationship may be seen in Figure 6.

Perhaps the most important aspect of deep groundwater salinity to deep borehole disposal is the value of the density gradient. Steeper gradients would result in more dramatic stifling of convective flows, while more gradual changes would likely provide less resistance to radionuclide transport. The above figure shows a wide range of slopes among the projected density curves. As expected, the relationships based upon exponential and polynomial TDS with depth relationships have the highest gradients before 2000m. The other curves more slowly reach their maximum values of density determined by the maximum of the density with TDS relationship used at a TDS of 350g/L.

The most extreme density curve results from combining Equations (1) and (7). The maximum density of 1296g/L is reached at 1600m. The most conservative relationship results from Equations (3) and (8), reaching a density of 1192g/L at 4900m. The large differences in both density at 350g/L and depth at which this salinity is reached highlight the need for more precise models of both variables.

Some important limitations include the lack of data below 1800m, the simplifications made, and the fits to the data. Certainly, the plentiful figures for TDS at low depths give credence to exponential or polynomial curves for TDS as explained in Section 4. Data from deeper depths such as the KTB borehole in Germany and the Kola borehole also support the TDS limit (saturation)

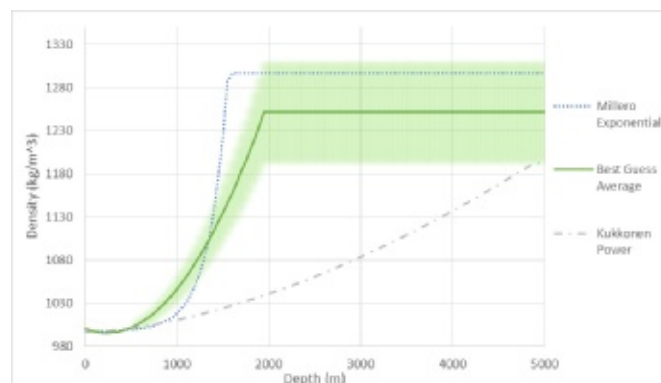


Figure 7. Maximum, minimum, and best guess density with depth curves

assumption (Frape et al., 2003; Smellie, 2004). Therefore it is valid to estimate a polynomial relationship between TDS and depth until 350g/L is reached. From there, utilizing the simplification discussed in Equation (6), we arrive at a best guess curve by combining Equations (2) and (7) into (12). The maximum, minimum, and best guess curve with spread are plotted in Figure 7. This spread accounts for variations in ion composition and their effects on density, not variations in concentration.

$$\rho = (7.08 \times 10^{-4} \pm 1.5 \times 10^{-4}) \times (0.1234 \times \text{Depth(m)}^2 - 59.419 \times \text{Depth(m)} + 5844.6) + \rho_{ref} \quad (12)$$

Valid for depth <1950m. Below this depth, $\rho = \rho_{ref} + 200.437 \pm 53.88$.

Future work

The site specific density gradient will have an enormous impact on thermal convection in a deep borehole repository. Preliminary curve fits suggest that both the maximum and best guess density curves have the potential to offset very large density decreases due to temperature (~150 °C), which in turn would prevent convective flows which could carry radionuclides upward. Depths shallower than 2000m are well accounted for by the data, at least in the Canadian Shield, and it is at these depths above the disposal zone where convection effects are perhaps most important. Certainly, more sophisticated models are necessary to test the validity of these estimations at some of the great depths relevant to deep geological repositories.

However, in order to quantify these potential effects, more work must be done both to narrow the spread of the formulations derived in this report, and to model the counterbalancing effects of temperature, pressure, and salinity on density. Therefore, more studies of potential deep borehole sites are called for, along with analyses of fluid flow based both upon first principles and simulation. An increased understanding of the natural

salinity gradient and its effect on fluid density and flow will be necessary in order for wise choices to be made concerning spent nuclear fuel disposal.

Acknowledgments

I would like to thank Professor Michael J. Driscoll for the opportunity to work on this project along with the tremendous assistance and support he has offered. Additionally, Ethan Bates has been remarkably generous with his guidance, time, and assistance. Furthermore, Nazar Lubchenko, Emilio Baglietto, and Jacopo Buongiorno have been extremely gracious with their time and expertise. Financial support was provided by the MIT UROP program and the Department of Nuclear Science and Engineering.

References

1. American Chemical Society (2006) (2006). In Reagent Chemicals: Specifications and Procedures: American Chemical Society Specifications, (Oxford University Press), p. 242.
2. Arnold, B.W., and Hadgu, T. (2013). Thermal-Hydrologic Modeling of a Deep Borehole Disposal System. In Proposed for Presentation at the International High-Level Radioactive Waste Management Conference Held April 28 - May 2, 2013 in Albuquerque, NM.,.
3. Chaudhuri, A., Rajaram, H., and Viswanathan, H. (2008). Alteration of fractures by precipitation and dissolution in gradient reaction environments: Computational results and stochastic analysis. *Water Resour. Res.* 44, W10410.
4. Fournier, R.O., and Rowe, J.J. (1977). The solubility of amorphous silica in water at high temperatures and high pressures. *American Miner.* 62, 1052–1056.
5. Frape, S.K., Fritz, P., and McNutt, R.H. (1984). Water-rock interaction and chemistry of groundwaters from the Canadian Shield. *Geochim. Cosmochim. Acta* 48, 1617 – 1627.
6. Frape, S.K., Blyth, A., Blomqvist, R., McNutt, R.H., and Gascoyne, M. (2003). 5.17 - Deep Fluids in the Continents: II. Crystalline Rocks. In *Treatise on Geochemistry*, Editors-in-Chief: Heinrich D. Holland, and Karl K. Turekian, eds. (Oxford: Pergamon), pp. 541–580.
7. Fritz, P., and Frape, K. (1982). Comments on the ^{18}O and ^2H , and Chemical Composition of Saline Groundwaters on the Canadian Shield. In *Isotope Studies of Hydrologic Processes*, (Northern Illinois University Press),.
8. Gascoyne, M. (2004). Hydrogeochemistry, groundwater ages and sources of salts in a granitic batholith on the Canadian Shield, southeastern Manitoba. *Appl. Geochem.* 19, 519–560.
9. Hartley, L., and AB, S. kärnbränslehantering (2006). Groundwater Flow and Transport Modelling During the Temperate Period for the SR-Can Assessment: Laxemar Subarea - Version 1.2 (SKB).
10. Haug, M.D., Barbour, S.L., and Longval, P. (1988). Design and construction of a prehydrated sand-bentonite liner to contain brine. *Can. J. Civ. Eng.* 15, 955–963.
11. Kukkonen, I.T. (1995). Thermal aspects of groundwater circulation in bedrock and its effect on crustal geothermal modelling in Finland, the central Fennoscandian Shield. *Heat Flow Therm. Regimes Cont. Lithosphere* 244, 119–136.
12. Laliberte, M., and Cooper, E. (2004). Model for Calculating the Density of Aqueous Electrolyte Solutions. *J. Chem. Eng. Data* 49, 1141–1151.
13. Millero, F.J., Chen, C.-T., Bradshaw, A., and Schleicher, K. (1980). A new high pressure equation of state for seawater. *Deep Sea Res.* 27, 255–264.
14. Oberlander, P.L. (1989). Fluid Density and Gravitational Variations in Deep Boreholes and Their Effect on Fluid Potential. *Ground Water* 27, 341–350.
15. Park, Y.-J., Sudicky, E.A., and Sykes, J.F. (2009). Effects of shield brine on the safe disposal of waste in deep geologic environments. *Adv. Water Resour.* 32, 1352 – 1358.
16. Slovic, P., Flynn, J.H., and Layman, M. (1991). Perceived Risk, Trust, and the Politics of Nuclear Waste. *Science* 254, 1603–1607.
17. Smellie, J. (2004). Recent Geoscientific Information Relating to Deep Crustal Studies (SKB).
18. Weres, O., Yee, A.W., and Tsao, L. (1979). Kinetic equations and type curves for predicting the precipitation of amorphous silica from geothermal brines. 1979 SPE ALME Int. Symp. Oilfield Geotherm. Chem.
19. Zhang, H.-L., Chen, G.-H., and Han, S.-J. (1997). Viscosity and Density of $\text{H}_2\text{O} + \text{NaCl} + \text{CaCl}_2$ and $\text{H}_2\text{O} + \text{KCl} + \text{CaCl}_2$ at 298.15 K. *J. Chem. Eng. Data* 42, 526–530.



Never lost your curiosity?

MAKE GREAT THINGS HAPPEN

Opportunities for research scientists and professionals: You have always strived to sustainably improve people's lives? Contribute to exciting projects in cell biology, protein research or in one of our high-growth therapeutic areas – cancer, neurodegenerative as well as autoimmune and inflammatory diseases, infertility and hormone disorders. We offer excellent development perspectives and exceptionally quick decision making processes you will only find in mid-sized companies like ourselves. Join us and take part in shaping our global business. Ready to tread new paths?

EMD is the North America name of Merck KGaA, Darmstadt, Germany. With more than 300 years of progress and about 38,000 employees in over 60 countries, we are leading in pharma, chemicals and life sciences. With passion, dedication and innovative ideas, we pursue one global goal: to improve people's quality of life.

Like to join in? Welcome to the team!

come2emd.com



IN A FASTER FORWARD WORLD

"Shaping the future of the Internet" could be your job description.



The Boston Globe
**TOP PLACES
TO WORK 2012**

TOP 25 COMPANIES
for Career Opportunities
glassdoor.com

NASDAQ-100

STANDARD
& POOR'S 500

Pushing the limits of what's possible. It's what we do every day at Akamai for leading brands like Standard Chartered Bank, Home Depot, and Apple. And it's the reason why the best and brightest choose to work here. A place where they are free to innovate, collaborate and shape how the world lives, works and plays.

Ready to create an exciting future? Then join us at jobs.akamai.com



Akamai Technologies is an Affirmative Action, Equal Opportunity employer (M/F/D/V) that values the strength that diversity brings to the workplace. ©2013 Akamai Technologies, Inc. The Akamai logo is a registered trademark of Akamai Technologies, Inc. All Rights Reserved.